Adv Polym Sci (2005) 175: 257–298
DOI 10.1007/b100117

Microemulsion Polymerizations and Reactions

Pei Yong Chow (✉)[1] · Leong Ming Gan[2]

[1] Institute of Bioengineering and Nanotechnology, 31 Biopolis Way, The Nanos, #04–01, 138669 Singapore
echow@ibn.a-star.edu.sg
[2] Institute of Materials Research & Engineering, 3 Research Link, 117602 Singapore
lm-gan@imre.a-star.edu.sg

Abstract This review describes how the unique nanostructures of water-in-oil (W/O), oil-in-water (O/W) and bicontinuous microemulsions have been used for the syntheses of some organic and inorganic nanomaterials. Polymer nanoparticles of diameter approximately 10–50 nm can easily be obtained, not only from the polymerization of monomers in all three types of microemulsions, but also from a Winsor I-like system. A Winsor I-like system with a semi-continuous process can be used to produce microlatexes with high weight ratios of polymer to surfactant (up to 25). On the other hand, to form inorganic nanoparticles, it is best to carry out the appropriate chemical reactions in W/O- and bicontinuous microemulsions.

Recent developments in the cross-polymerization of the organic components used in bicontinuous microemulsions ensure the successful formation of transparent nanostructured materials. Current research into using polymerizable bicontinuous microemulsions as a one-pot process for producing functional membranes and inorganic/polymer nanocomposites is highlighted with examples.

Keywords Microemulsion polymerization · Microemulsion reaction · Water-in-Oil (W/O) microemulsion · Oil-in-Water (O/W) microemulsion · Bicontinuous microemulsion · Functional membranes and inorganic/polymer nanocomposites

Abbreviations

AN	Acrylonitrile
AA	Acrylic acid
AM	Acrylamide
APTAC	2-acrylamido-2-propane trimethylammonium chloride
AUTMAB	(Acryloyloxy)-undecyltrimethylammonium bromide
AUDMAA	(Acryloyloxy)-undecyldimethylammonioacetate
AIBN	Azobisisobutyronitrile
AOT	1,4-Bis(2-ethylhexyl)sulfosuccinate sodium salt
APS	Ammonium persulfate
BL	γ-butyrolactone
BUA	Butylacrylate
C_1-PEO-C_{11}-MA-40	ω-methoxypoly(ethylene oxide)$_{40}$-undecyl-α-methacrylate
CTAB	Cetyltrimethylammonium bromide
DMC	Dimethyl carbonate
DTAB	Dodecyltrimethylammonium bromide
EGDMA	ethyleneglycol dimethacrylate
EC	Ethylene carbonate
HC	Hydrocarbon
HA	Hydroxyapetite
HEMA	2-hydroxylethylmethacrylate
MADQUAT	2-Methacryloyloxyethyltrimethyl ammonium chloride
MMA	Methyl methacrylate
NaA	Sodium acrylate
NaAMPS	Sodium-2-acrylamido-2–2-methylpropane sulfonate
NaSS	Sodium styrenesulfonate
NIPAM	*N*-isopropylacrylamide
NP	Poly(oxyethylated alkylphenyl ether)
OTAC	Octyldecyltrimethylammonium chloride
PC	Propylene carbonate
PMMA	Poly(methyl methacrylate)
PNIPAM	Poly(*N*-isopropylacrylamide)

PS	Poly(styrene)
SDS	sodium dodecyl sulfate
SEAAU	Sodium 11-(*N*-ethylacrylamido)-undecanoate
St	Styrene
TEM	Transmission electron microscope
THFM	Tetrahydrofurfuryl methacrylate
TTAB	Tetradecyltrimethylammonium bromide
VA	Vinyl acetate
VBSLi	4-Vinylbenzene sulfonate, lithium salt

1 Introduction

Microemulsions are transparent liquid systems consisting of at least ternary mixtures of oil, water and surfactant. Sometimes a cosurfactant is needed for the formation of a thermodynamically-stable microemulsion. A transparent microemulsion is, in fact, heterogeneous (nanostructured) on a molecular scale. Microemulsion domains fluctuate in size and shape and undergo spontaneous coalescence and break-up [1]. They can exhibit water continuous and bicontinuous structures, with typical equilibrium domain sizes ranging from about 10 to 100 nm [2]. The transparent microemulsions can be in the form of nano-globules of oil-swollen micelles dispersed in the water continuous phase as oil-in-water (O/W) microemulsions, or water-swollen micellar globules dispersed in oil as water-in-oil (W/O) microemulsions. In between the regions of O/W and W/O microemulsions, there may also exist a composition region of bicontinuous (sponge-like structure) microemulsions [3], whose oil and water domains are randomly dispersed in two phases, as can be seen from the sketched phase diagram of Fig. 1.

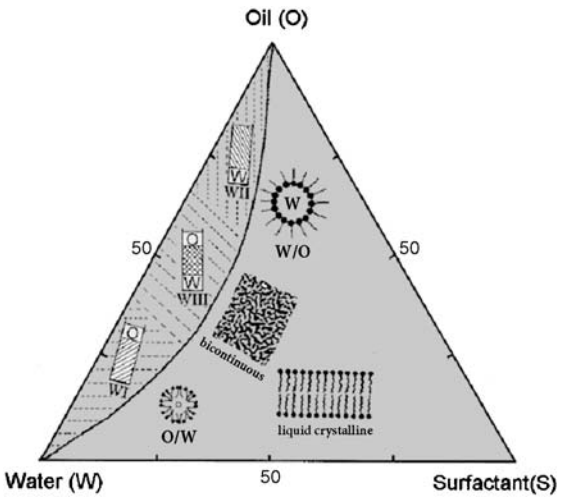

Fig. 1 Illustration of some phase equilibria encountered in multicomponent systems

In addition to single phase microemulsions, several phase equilibria known as Winsor systems [4] are also shown at low surfactant concentrations. A Winsor I (WI) system consists of an O/W microemulsion that is in equilibrium with an oil phase, while a Winsor II (WII) system is a W/O microemulsion in equilibrium with an aqueous phase. A WIII system has a middle phase (bicontinuous) microemulsion that coexists with both oil and aqueous phases.

When a single chain anionic surfactant (such as sodium dodecyl sulfate, SDS) is used, it generally requires a cosurfactant for the formation of a microemulsion. A cosurfactant may not be needed to form a microemulsion if nonionic surfactant(s), certain types of cationic surfactants, or double-chain surfactants such as sodium 1,4-bis(2-ethylhexyl)sulfosuccinate (Aerosol OT or simply AOT) are used.

Due to the enormous inner surfaces of the nanostructures of W/O and O/W globular microemulsions, they can provide novel reaction sites for some inorganic/organic reactions and polymerizations. Nano-sized particles of inorganic materials are generally prepared in W/O microemulsion, and microlatexes (d<50 nm) of polymers from both O/W- and W/O-microemulsion polymerizations. The recently developed approach of using polymerizable surfactants in bicontinuous microemulsions also enables the syntheses of transparent nanoporous polymeric materials and nanocomposites. Hence, microemulsions have been used as novel chemical nanoreactors for producing nanophase materials such as polymer latexes [5, 6], inorganic particles [7], and industrially useful materials [8]. This review relates the development of microemulsion polymerizations and reactions to the formation of nanostructured materials.

2
Polymerizations in Globular and Bicontinuous Microemulsions for Producing Microlatexes

Over the past two decades, free radical polymerization studies have mainly been carried out in globular microemulsions (both O/W microemulsions and W/O microemulsions, also known as inverse microemulsions). Each milliliter of the globular microemulsion usually contains 10^{15}–10^{17} W/O- or O/W nanosized (5–10 nm in diameter) droplets (globules). The enormous number of nano-globules are potential loci for fast polymerization, producing microlatex particles much less than 50 nm in diameter. Though small polymer particles, molecular weights exceeding one million can easily be obtained from these polymerization systems. Most of the microemulsion polymerization studies [5] have dealt with hydrophobic monomers, such as styrene (St) or methyl methacrylate (MMA), within oil cores of O/W microemulsions [9] and with the polymerization of water-soluble monomers, such as acrylamide (AM), within aqueous cores of inverse microemulsions [10, 11]. For both O/W and inverse microemulsion systems, the amount of monomer was usually restricted to less than 10 wt% with respect to the total weight of microemulsion. Moreover,

higher amounts of surfactant (5–15 wt%) were normally needed for the stability of the polymerization. For those microemulsions requiring a cosurfactant, the compatibility between the cosurfactant and the polymers formed becomes an issue. For instance, if styrene is polymerized within an O/W microemulsion that contains an alcohol cosurfactant, this alcohol will not dissolve polystyrene. However, this is not the case for the polymerization of acrylamide (AM) in alcohol-free inverse microemulsion.

2.1 Inverse Microemulsion Polymerization

The polymerization of a water-soluble monomer such as AM, acrylic acid (AA), sodium acrylate (NaA), or 2-hydroxyethylmethacrylate (HEMA), can be carried out easily in inverse microemulsion or/and bicontinuous microemulsion. These water-soluble monomers also act as cosurfactants, increasing the flexibility and the fluidity of the interfaces, which enhances the solubilization of the monomer. A cosurfactant effect during the polymerization of vinyl acetate in anionic microemulsions has also been reported [12].

Candau and co-workers were the first to address the issue of particle nucleation for the polymerization of AM [13, 14] in an inverse microemulsion stabilized by AOT. They found that the particle size of the final microlatex (d~20–40 nm) was much larger than that of the initial monomer-swollen droplets (d~5–10 nm). Moreover, each latex particle formed contained only one polymer chain on average. It is believed that nucleation of the polymer particle occurs for only a small fraction of the final nucleated droplets. The non-nucleated droplets also serve as monomer for the growing particles either by diffusion through the continuous phase and/or by collisions between droplets. But the enormous number of non-nucleated droplets means that some of the primary free radicals continuously generated in the system will still be captured by non-nucleated droplets. This means that polymer particle nucleation is a continuous process [14]. Consequently, each latex particle receives only one free radical, resulting in the formation of only one polymer chain. This is in contrast to the large number of polymer chains formed in each latex particle in conventional emulsion polymerization, which needs a much smaller amount of surfactant compared to microemulsion polymerization.

The polymerization of acrylamide (AM) and the copolymerization of acrylamide-sodium acrylate in inverse microemulsions have been studied extensively by Candau [10, 11, 13–15], Barton [16, 17], and Capek [18–20]. One of the major uses for these inverse microlatexes is in enhanced oil recovery processes [21]. Water-soluble polymers for high molecular weights are also used as flocculants in water treatments, as thickeners in paints, and retention aids in papermaking.

2.2 Bicontinuous Microemulsion Polymerization

The polymerization of AM in inverse microemulsions originally required a high weight ratio of surfactant/monomer. This high ratio was subsequently drastically reduced by polymerizing water-soluble monomers in nonionic bicontinuous microemulsions [10, 22]. Besides AM, other water-soluble monomers investigated were sodium acrylate [23], sodium 2-acrylamido-2–2-methylpropane sulfonate [24] (NaAMPS, CH_2=CHCONHC$(CH_3)_2CH_2SO_3Na$) and 2-methacryloyloxyethyltrimethylammonium chloride [25] (MADQUAT, CH_2=C(CH_3)COO$CH_2CH_2H(CH_3)_3Cl$). This type of polymerization has been extended to syntheses of copolymers that possess both positively and negatively charged moieties along the macromolecular backbone (polyampholytes). High charge density polyampholytes can be formed from the microemulsion copolymerization [25] of NaAMPS and MADQUAT. Polymerization of water-soluble monomers in bicontinuous microemulsions produced transparent microlatexes [26] with particle sizes (50–100 nm) that remain unchanged for years.

Microemulsion formulation was further optimized by Candau [27] using cohesive energy ratio (CER) and hydrophile-lipophile balance (HLB) concepts. The best formulation was obtained for high HLB values (8–11) using a blend of nonionic surfactants. This favors microemulsions with bicontinuous structures in the presence of AM and NaAMPS or AM and NaA. The process yielded clear, stable microlatexes of moderate particle size (d<100 nm) for high molecular weight copolymers up to 25 wt% solids. High-solid content (~30 wt%) of water-soluble poly(vinyl acetate) latexes [28] could also be obtained by the multi-stage addition of monomer to a latex pre-produced by the polymerization of 3 wt% vinyl acetate in three-component microemulsions stabilized by low concentration of AOT (<1 wt%). These microemulsion-made latexes contained latex particles two to three times smaller than those obtained by emulsion polymerization.

Syntheses of thermosensitive polyampholytes by polymerization in bicontinuous microemulsions have also been studied by Candau's group [29, 30] recently. Poly(*N*-isopropylacrylamide) (PNIPAM) exhibits a well-defined lower critical solution temperature (LCST) in water around 32 °C, and it is the most extensively studied temperature-responsive polymer. The microemulsion contained three-monomer-mixtures, namely, *N*-isopropylacrylamide (NIPM, neutral), NaAMPS (anionic), and 2-acrylamido-2-propanetrimethylammonium chloride (APTAC, cationic). Bicontinuous microemulsions were produced in an HLB domain ranging between around 10.6 and 11.3 using a blend of nonionic surfactants. After polymerization, it formed thermosensitive polymers, namely NIPAM-based polyelectrolytes and polyampholytes. The final products consisted of stable and clear microlatexes of small particle size containing up to 20 wt% high molecular weight copolymers. In order to overcome the high surfactant-to-monomer ratio used, they performed the polymerization by a

semi-continuous process that reduced the surfactant content required to stabilize the final microlatexes by more than 40%.

2.3 Polymerization in Oil-in-Water Microemulsions

The main difficulty encountered by most researchers working on cosurfactant-O/W microemulsion polymerization over the past decade [31–36] is the instability of microlatex produced from systems that use lower weight ratios (<1) of surfactant to monomer for a higher content of polymer (>8 wt%). The instability of the resulting microlatexes may be due to the incompatibility between the higher content of polymer formed and the cosurfactant [37]. The polymerization of a hydrophobic monomer in a ternary O/W microemulsion without a cosurfactant was first reported in 1989 by Ferrick et al [38]. This spurred a new interest in systematic polymerization studies for cationic O/W microemulsions [39–42]. The cationic surfactants can be dodecyltrimethylammonium bromide (DTAB), tetradecyltrimethylammonium bromide (TTAB), or cetyltrimethylammonium bromide (CTAB). Nonionic surfactants were also used in ternary O/W microemulsions for the polymerization of styrene and methylmethacrylate (MMA) [43] and anionic AOT microemulsion for the polymerization of tetrahydrofurfuryl methacrylate (THFM) [44]. Anionic SDS ternary O/W microemulsions have also been used to study the polymerization of butylacrylate (BUA) [45, 46], alkyl acrylates [47], and the copolymerization of BUA with acrylonitrile [48]. All of the microemulsion polymerizations produced stable microlatexes with particle sizes ranging from 20 to 60 nm in diameter. However, these ternary O/W microemulsions usually required a high surfactant concentration (7–15 wt%) to solubilize a relatively low monomer content of less than 10 wt%. These conventional O/W microemulsion polymerization recipes call for the use of at least an equal amount of surfactant and monomer, which makes the polymerization and surfactant removal processes prohibitively expensive. Nevertheless, there have been a few studies in which the formulation has been modified from these polymerization conditions in order to dramatically reduce the use of surfactant, as we will discuss in the next section.

It is generally accepted that an O/W microemulsion polymerization proceeds via a continuous particle nucleation mechanism, as in the case of inverse microemulsion polymerization [14]. The particle nucleation of polymer is generally postulated to occur in microemulsion droplets (micellar nucleation mechanism) for less water-soluble monomers, such as styrene and BUA. Homogeneous nucleation for this type of monomer may be insignificant because of an extremely large number of microemulsion droplets ($\sim 10^{16}$–10^{17} m/L) that can effectively capture the free radicals generated. The primary radicals generated in the aqueous phase probably react first with some dissolved monomers in the aqueous phase to form oligomeric radicals of higher hydrophobicity. These oligomeric radicals can then be captured more favorably by microemulsion

droplets. Therefore, the newly formed latex particles continue to grow in the microlatex through the constant supply of monomer from nucleated droplets until the chain in the particle is terminated by chain transfer to monomer [42, 49, 50]. However, Kaler's group recently consistently obtained very high molecular weights of ~15×10^6 Da for styrene O/W microemulsion polymerizations [51]. Such molecular weights are considerably higher than those typically obtained via free-radical polymerizations. In the free-radical polymerization of styrene, the chain transfer to monomer is limited and hence can only produce molecular weights of up to ~2×10^{-6} Da, as suggested by the most recent measurements of chain-transfer constants by Kukulj et al [52]. Therefore, the diffusion-limited exit of monomer radicals to the aqueous phase coupled with chain transfer to polymer are probable reasons for the enhanced molecular weight of polystyrene [51].

In contrast to emulsion polymerization, the reaction kinetics of microemulsion polymerization is characterized by two polymerization rate intervals; the interval of constant rate characteristic of emulsion polymerization is missing [42, 49, 53], as shown in Fig. 2. Polymer particles are generated continuously during the reaction by both micellar and homogeneous mechanisms. As the solubility of the monomer in the continuous domain increases, homogeneous

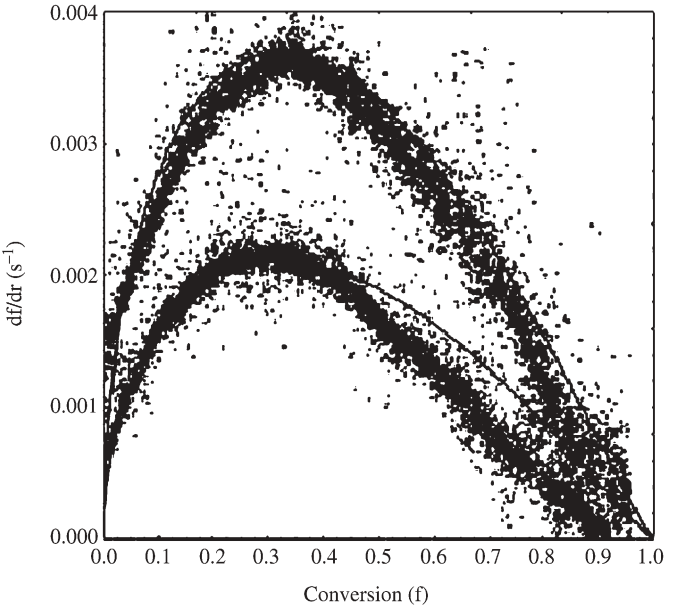

Fig. 2 Experimental and model rate versus conversion profiles for the polymerization of hexylmethacrylate in a microemulsion stabilized by the surfactant DTAB. The two curves are for initiator concentrations of 0.045 wt% (top) and 0.015 wt% (bottom) relative to the amount of monomer in the microemulsion. The solid lines are predictions from the Morgan model [56]

nucleation becomes more important [54]. In O/W microemulsion polymerization, monomer partitioning between polymer particles and uninitiated micelles via diffusion through the aqueous phase determines the concentration of monomer at the polymerization loci. This partitioning plays an important role in determining polymer particle formation and growth [55–57]. The rate of polymerization initially increases to a maximum around 20–25% of total monomer conversion (Interval I) and then decreases on further polymerization (Interval II). This is generally interpreted as indicating that the particle nucleation occurs mainly in Interval I, and polymer growth occurs in Interval II. The decreased polymerization rate in Interval II is due to the progressively depletion of monomer in the latex particles.

The growth pattern for PMMA particles was found to be different from that for styrene polymerization in ternary cationic microemulsions [58, 59] containing either TTAB, TTAC, CTAB or OTAC (octyldecyltrimethylammonium chloride). For the MMA microemulsions, the average hydrodynamic particle radius (R_h) increased continuously from about 20 to 50 nm during the polymerization. The improved interactions between the cosurfactant MMA and the cationic surfactant at interfaces may restrict the swelling of MMA-swollen PMMA particles. Hence a gradual increase in the sizes of the PMMA particles during polymerization was observed, as expected [59]. However, this was not the case for the weaker interaction between styrene and a cationic surfactant in the corresponding microemulsion. The maximum swelling of PS particles by styrene monomer, and hence the largest R_h, was attained during the early stage of polymerization (4–7% polymer conversion) [58]. As the styrene polymerization continued, R_h generally decreased due to the diminishing styrene concentration in the swollen PS particles. For some polymerized MMA-micro emulsions, particle sizes might increase significantly towards the final stage of polymerization. The agglomeration of some PMMA latex particles stabilized by TTAB was evidenced by the prolonged heating (long term storage) of microlatexes [60] at 60 °C, as shown in Fig. 3. Cationic surfactants with larger carbon chain lengths, such as OTAC or CTAB, form thicker interfacial layers which prevent latex flocculation through steric stabilization. It should be noted that the stability of PS microlatex was not affected by the alkyl chain length of the cationic surfactant due to stronger surfactant adsorption on the surface of PS particles than on PMMA particles [60]. Indeed, it is known that surfactant adsorption on the latex/water surface decreases with increasing polymer polarity [61].

Core-shell nanoparticles can also be fabricated using microemulsions. This was performed using a two-stage microemulsion polymerization beginning with a polystyrene seed [62]. Butyl acrylate was then added in a second step to yield a core-shell PS/PBA morphology. The small microlatex led to better mechanical properties than those of similar products produced by emulsion polymerization. Hollow polystyrene particles have also been produced by microemulsion polymerization of MMA in the core with crosslinking of styrene on the shell. After the synthesis of core-shell particles with crosslinked PS shells, the PMMA core was dissolved with methylene chloride [63]. The direct cross-

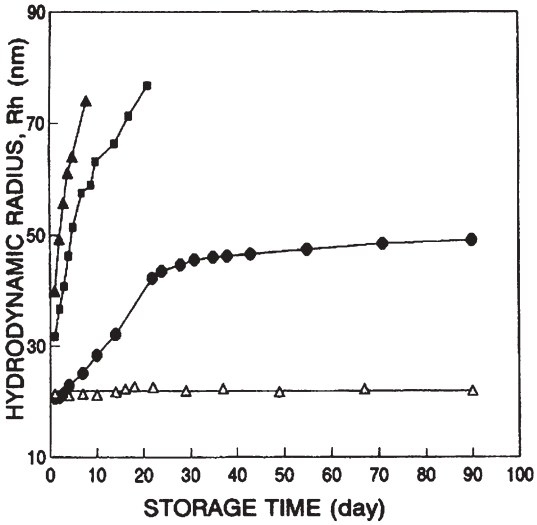

Fig. 3 Changes in PMMA particle size during long term storage at 60 °C for microlatexes stabilized by different surfactants: (filled triangles) TTAB; (filled squares) TTAC; (filled circles) CTAB; (empty triangles) OTAC

linking polymerization of styrene at the interfaces of isooctane microdroplets of microemulsion also produced hollow nanocapsules [64].

2.4 Microemulsion Polymerization for Microlatexes with High Polymer-to-Surfactant Weight Ratios

A major drawback of conventional microemulsion polymerization is the high surfactant-to-monomer ratio usually needed to form the initial microemulsion. Surfactant can be used more efficiently in semi-continuous or fed polymerization processes. Several polymerization cycles can be run in a short period of time by stepwise addition of new monomer. After each cycle of monomer addition, most of the surfactant is still available to stabilize the growing hydrophobic polymer particles, or to forms microemulsion again when a polar monomer is used. For instance, in the polymerization of vinyl acetate (VA) by a semi-continuous microemulsion process [21], latexes with a high polymer content of about 30 wt% were obtained at relatively low AOT concentrations of about 1 wt%. Moreover, their particle sizes and molecular weights were much smaller than those obtained by conventional emulsion polymerization.

A new system associated with an O/W microemulsion for styrene polymerization of up to 15 wt% solids at about 1 wt% DTAB was first reported [65] in 1994. This new two-phase system is rather similar to a Winsor I system, as depicted in Fig. 1; an organic phase containing small portions of water and surfactant in equilibrium with an O/W microemulsion in the bottom phase.

The new system consists of a pure styrene upper phase placed on top of a ternary O/W microemulsion. Strictly speaking, this new system is not identical to the Winsor I system. Hence the new polymerization system has been referred as a "Winsor I-like" system, which can be prepared by simply topping up a ternary O/W microemulsion with hydrophobic monomer without disturbing the microemulsion phase. Styrene polymerization took place only in the initial ternary microemulsion containing 0.5–1.0 wt% styrene, 1.0 wt% DTAB and a redox initiator of ammonium persulfate/tetramethylethylenediamine (APS/TMEDA). The upper styrene phase acted only as a monomer reservoir to continuously supply monomer to the polymerization loci in the lower microemulsion phase through diffusion without stirring. PS particles initially formed in the microemulsion phase became the seed for the further growth of PS particles to a more uniform size, up to about 80 nm in diameter. Therefore, microlatexes of about 15 wt% PS could be obtained using only 1 wt% DTAB. It should also be noted that the Winsor I-like system with a small amount of monomer in the upper phase becomes a milky emulsion on stirring. But this milky emulsion will transform into a transparent or bluish microlatex after polymerization.

The polymerization rate of the Winsor I-like system was very slow due to the low monomer diffusion rate through the limited interface to the polymerization loci for the unstirred system. In order to increase the interfacial areas for the infusion of monomer to the polymerization loci, hollow fiber monomer feeds were later used to polymerize not only styrene, but also MMA and butylacrylate [66]. Such a set-up using continuous monomer feeding via a hollow-fiber is shown in Fig. 4. About 100 polypropylene (PP) hollow fibers (pore size 70 nm) were bundled together. One of the openings of the hollow-fiber bundle was used for monomer feeding and the other end was sealed with epoxy resin. The initial microemulsion usually consisted of 0.5 wt% styrene or BA, or 2 wt% MMA, 1 wt% CTAB or 1.5 wt% SDS together with 0.2 wt% 1-pentanol, 4 mM equimolar redox initiator (APS/TMEDA), and water to make it up to 100 wt%. After polymerization of the microemulsion for about 15 min at room temperature with about 97–98% conversion, the additional monomer was then continuously introduced to the polymerization system via the infusion of monomer from hollow fibers connected to monomer reservoir. The rate of monomer infusion into the microemulsion could be regulated by the external nitrogen pressure applied to the monomer reservoir. The slow bubbling by nitrogen gas into the polymerizing microemulsion was to ensure homogeneous mixing. When the infusion rate of monomer was optimal, latex particles would grow to more uniform sizes at the expense of forming secondary particles via homogeneous nucleation. This method was able to produce almost uniform microlatexes of various sizes (15–65 nm) at high polymer/surfactant weight ratios up to about 15 with high molecular weights (10^6 g/mol) within 2–3 h.

Though the continuous addition of monomer via hollow fibers into a Winsor I-like system is rather novel, it is not as convenient as the drop-wise addition of monomer under a semi-continuous process. Ming et al [67, 68]

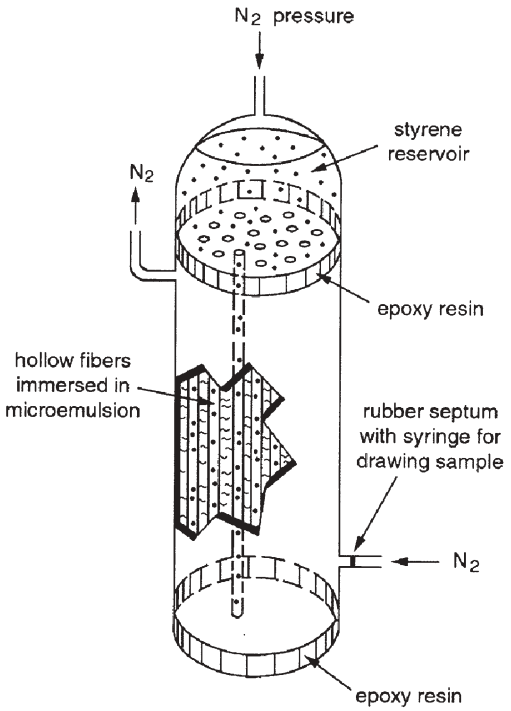

Fig. 4 Schematic presentation of the set-up (not to scale) for the polymerization of monomer in a microemulsion via hollow-fiber feeding of additional monomer

slightly modified the Winsor I-like method by directly adding monomer very slowly to pre-polymerized ternary microemulsions for producing microlatexes of PS, PMMA, poly(butyl methacrylate), or poly(methacrylate) (PMA). With 1 wt% DTAB, 24 wt% PMMA microlatexes of 33–46 nm in size were obtained. They showed that this semi-continuous process was very effective for producing small microlatexes (15 nm) containing up to 30 wt% PMA at a high PMS to SDS weight ratio of 25:1. The semi-continuous process works at the monomer-starved condition to ensure that no empty micelles exist during polymerization.

The polymerization of styrene in Winsor I-like systems by semi-continuous feeding of monomer stabilized by either DTAB, TTAB or CTAB has been systematically investigated by Gan and coworkers [69a]. Rather monodisperse polystyrene microlatexes of less than 50 nm with molecular weights of over one million were obtained at a polymer/surfactant weight ratio of 14:1. The Winsor I-like (micro)emulsion polymerization of styrene stabilized by non-ionic surfactant and initiated by oil-soluble initiators has also been reported very recently [69b]. The sizes of the large monomer-swollen particles decreased with conversion and they merged with growing particles at about 40–50% conversion.

High PMMA content (30–40%) microlatexes [70] stabilized with low concentrations of anionic SDS were also prepared by microemulsion polymeriza-

tion via semi-continuous feeding of MMA. The synthesis of monodisperse poly(dimethylsiloxane) microlatexes (<80 nm) [71] stabilized by several surfactants were also obtained at polymer/surfactant weight ratios of up to 3:1.

Nanosized polystyrene (PS) microlatexes stabilized by a mixture of cationic/cationic, anionic/anionic, or anionic/cationic surfactants of various types [72] with PS-to-surfactant weight ratios up to 10:1 have been synthesized by a semi-continuous microemulsion polymerization process. For cationic or anionic systems, spherical latex particles ranging from about 22 to 53 nm were produced almost linearly, independent of the weight ratio of the mixed surfactants of similar charges. High molecular weight (M_w) PS ranging from 1.1×10^6 to 1.9×10^6 g/mol could easily be obtained from all three systems. The present polymerization method allows one to synthesize nanoparticles of PS or other polymers with high polymer/surfactant weight ratios at some particle sizes that cannot be achieved with a single type of surfactant.

High polymer/surfactant weight ratios (up to about 15:1) of polystyrene microlatexes [73] have been produced in microemulsions stabilized by polymerizable nonionic surfactant by the semi-continuous process. The copolymerization of styrene with the surfactant ensures the long-term stability of the latexes. Nanosized PS microlatexes with polymer content (≤25 wt%) were also obtained from an emulsifier-free process [74] by the polymerization of styrene with ionic monomer (sodium styrenesulfonate, NaSS), nonionic comonomer (2-hydroxyethylmethacryalte, HEMA), or both. The surfaces of the latex particles were significantly enriched in NaSS and HEMA, providing better stabilization.

Nanoparticles of PS (M_w=1.0×10^6–3.0×10^6 mol^{-1}) microlatexes (10–30 nm) have also been successfully prepared from their respective commercial PS for the first time [75]. The dilute PS solutions (cyclohexane, toluene/methanol or cyclohexane/toluene) were induced to form polymer particles at their respective theta temperatures. The cationic CTAB was used to stabilize th microlatexes. The characteristics of these as-formed PS latex particles were quite similar to those obtained from the microemulsion polymerization of styrene as reported in literature. These microlatexes could also be grown to about 50 nm by seeding the polymerization of styrene with a monodisperse size distribution of D_w/D_n=1.08. This new physical method for preparing polymer nano-sized latexes from commercial polymers may have some potential applications, and therefore warrants further study.

3
Bicontinuous-Microemulsion Polymerization for Nanostructured Solid-Materials

Numerous attempts to prepare nanostructured materials by polymerization of suitable monomers (like MMA and styrene) in water-in-oil [76, 77] or oil-in-water [39, 51, 78–81] and bicontinuous microemulsion [27, 82–84] have been made. Polymeric materials were traditionally stabilized by non-polymerizable

surfactants, such as sodium dodecyl sulfate (SDS), and their polymerized microemulsions were usually found to be opaque and phase-separated. By incorporating polymerizable acrylic acid as co-surfactant in a microemulsion, stable transparent polymeric materials can be obtained but only at low solid contents (<15 wt%) [85]. However, the polymerized microemulsions did not reveal any microstructures when viewed by scanning electron microscope (SEM). But when SDS was replaced by a polymerizable surfactant, transparent nanoporous polymeric materials were obtained.

3.1 Nanostructured Polymers Produced by Bicontinuous-Microemulsion Polymerizations

There is increasing interest in the study of the formation of transparent nanoporous polymers (film or sheet) by bicontinuous-microemulsion polymerization [86–91a]. The real success of forming transparent solid polymers possessing various nanostructures arises from the polymerization of bicontinuous microemulsions containing a polymerizable surfactant with other monomers. The polymerizable surfactants are also known as "surfers" [91b], and they can be anionic sodium 11-(*N*-ethylacrylamindo)-undecanoate (SEAAU), cationic (acryloyloxy)-undecyltrimethylammonium bromide (AUTMAB), zwitterionic (acryloyloxy)-undecyldimethylammonioacetate (AUDMAA) or nonionic ω-methoxypoly(ethylene oxide)$_{40}$-undecyl-α-methacrylate (C_1-PEO-C_{11}-MA-40), as listed in Table 1. The polymerizable surfactants should not contain allylic hydrogens, to avoid active allylic chain transfer reactions.

The development of polymerizable microemulsions consisting of only three basic components (except a water component) for producing transparent solid polymers with nanostructure is a recent achievement [87]. For example, Fig. 5 shows the SEM micrograph of the fractured polymer prepared by the UV-initiated polymerization of a bicontinuous microemulsion consisting of 35 wt% water, 35 wt% AUDMAA and 30 wt% MMA. This micrograph reveals randomly distributed bicontinuous nanostructures of water channels and polymer domains. The widths of the bicontinuous nanostructures were about 40–60 nm. The sizes of the nanostructures can be readily reduced by adding 2-hydro-

Table 1 Some polymerizable surfactants that have been synthesized

Surfactant	Structure	CMC (mol l^{-1}, 25 °C)	Reference
SEAUU	CH_2=CHCON(C_2H_5)(CH_2)$_{10}$$COO^-Na^+$	4.2×10^{-5}	[92]
AUTMAB	CH_2=CHCOO(CH_2)$_{11}$-N^+(CH_3)$_3$$Br^-$	1.4×10^{-2}	[88]
AUDMAA	CH_2=CHCOO(CH_2)$_{11}$-N^+(CH_3)$_2$$CH_2COO^-$	9.3×10^{-3}	[87]
C_1-PEO-C_{11}-MA-40	CH_2=CHCOO(CH_2)$_{11}$-(OCH_2CH_2)$_{40}$$OCH_3$	6.6×10^{-5}	[93]

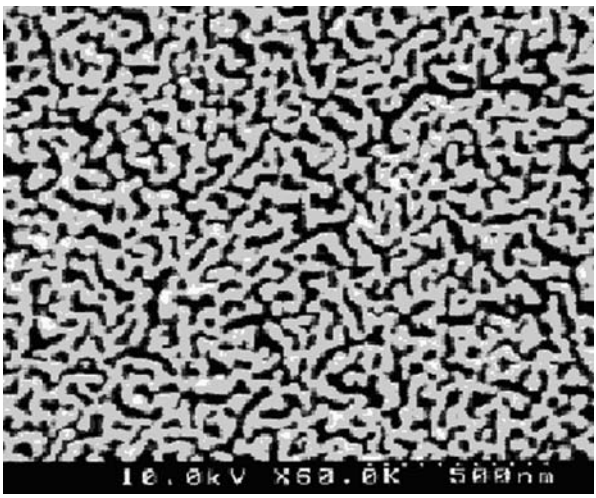

Fig. 5 SEM micrograph of a fractured polymer prepared by polymerization of a bicontinous microemulsion consisting of 35 wt% H_2O, 35 wt% AUDMAA and 30 wt% of MMA. The black and gray areas refer to water and polymer domains respectively

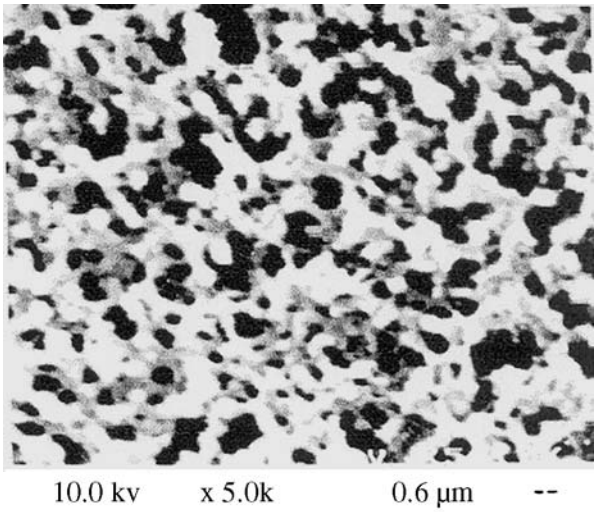

Fig. 6 SEM micrograph of a fractured polymer prepared by polymerization of a bicontinous microemulsion consisting of 30 wt% H_2O, 28 wt% AUTMAB, 38 wt% of MMA and 4 wt% HEMA. The black and gray areas refer to water and polymer domains respectively

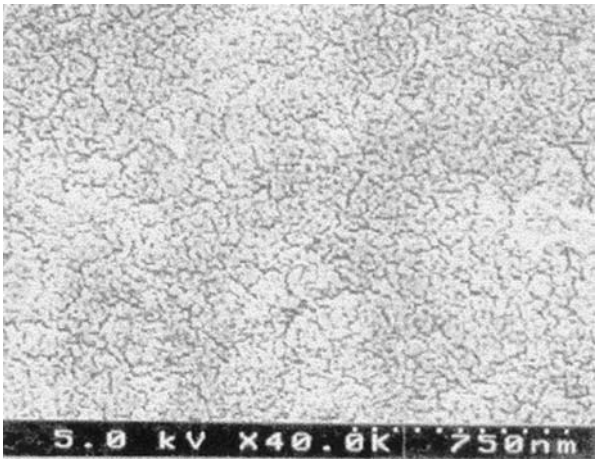

Fig. 7 SEM micrograph of a fractured polymer prepared by polymerization of a bicontinous microemulsion consisting of 40 wt% aqueous solution containing 3% NaCl, 33 wt% AUTMAB and 27 wt% of MMA. The black and gray areas refer to water and polymer domains respectively

xyethylmethacrylate (HEMA) or increased by adding 1–3 wt% NaCl solution, as shown in Figs. 6 and 7 [91a] respectively. In all of the bicontinuous microemulsions investigated, about 1 wt% of cross-linker ethyleneglycol dimethacrylate (EGDMA) was usually used to enhance the mechanical strengths of the polymers.

This type of cross-polymerization of all of the organic components (like MMA, HEMA and a polymerizable surfactant) in a bicontinuous microemulsion is an important area of recent development in microemulsion polymerization, which can be used to produce nanostructures of transparent polymer solids. The polymerization can be readily initiated using either redox or photo-initiators. The gel formation usually occurred within 20 minutes. The use of this novel type of microemulsion polymerization for preparing transparent inorganic-polymer nanocomposites in the form of films or sheets is emerging and exciting. However, very little published information about this type of nanocomposite is available, as will be described in the following sections.

3.1.1 Ion-Conductive Membranes

The development of transparent polymer electrolyte membrane from the bicontinuous-microemulsion polymerization of 4-vinylbenzene sulfonic acid lithium salt (VBSLi), acrylonitrile and a polymerizable non-ionic surfactant, ω-methoxypoly(ethylene oxide)$_{40}$-undecyl-α-methacrylate (C_1-PEO-C_{11}-MA-40) was reported in 1999 [94, 95]. The ionic conductivities of the polymer electro-

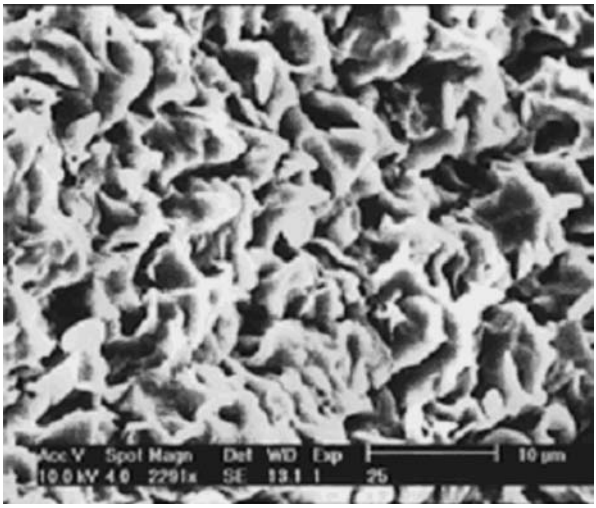

Fig. 8 SEM micrograph of the polymerized microemulsion solid, that contains the polymerizable non-ionic surfactant C_1-PEO-C_{11}-MA-40 [96], after ethanol extraction

lyte membranes were rather high, in the range of $(2–3)\times10^{-3}$ S/cm. This relatively high conductivity is attributed to the inclusion of the polymerizable ionic salt VBSLi and the existence of the interconnected aqueous channels in the polymerized bicontinuous network, which facilitate ionic conduction for the membrane electrolyte [94]. However, some unusual ionic conduction phenomena were also observed for these ion-containing membranes – large ions exhibited higher mobilities than smaller ones [95]. A possible explanation comes from the larger hydration shells of the lighter cations. This is further supported by the sharp drop in conductivity when the system is cooled below the freezing point of water.

The morphology of the microemulsion-polymerized solid after ethanol extraction, as revealed by SEM, is shown in Fig. 8. The extracted samples show globular microstructures and voids (pores). These pores might be derived from the interconnected water-filled voids generated from numerous coalescences of growing particles during polymerization.

The water in the membranes [96] could easily be replaced by polar organic solvents, such as BL, PC-EC, or EC-DMC, by immersion. The conductivities of the membranes decreased sharply (by about two orders of magnitude) with the use of organic solvents. After soaking these membranes in electrolyte solutions of 1 M $LiSO_3CF_3$/PC-EC, 1 M $LiBF_4$/BL, or 1 M $LiClO_4$/EC-DMC, their conductivities were restored to 10^{-3} S/cm [96]. This demonstrates that the water content in these microporous membranes can be freely exchanged for organic solvents or electrolyte solutions, indicating that they may be further developed as composite polymeric electrolytes for lithium/lithium ion rechargeable batteries.

3.1.2
Proton-Exchange Membranes

The bicontinuous-microemulsion polymerization technique has also been used to develop novel proton exchange membranes (PEM) for fuel cell evaluation [97]. A series of hydrocarbon-based membranes were prepared based on the formulation shown in Fig. 5, with additional ionic vinyl monomers such as VBSLi or bis-3-sulfopropyl-itaconic acid ester. After polymerization, the membranes were treated with dilute H_2SO_4 (0.5 M) to convert them to PEM membranes. The good performance of these PEM membranes in a single fuel cell is illustrated in Fig. 9.

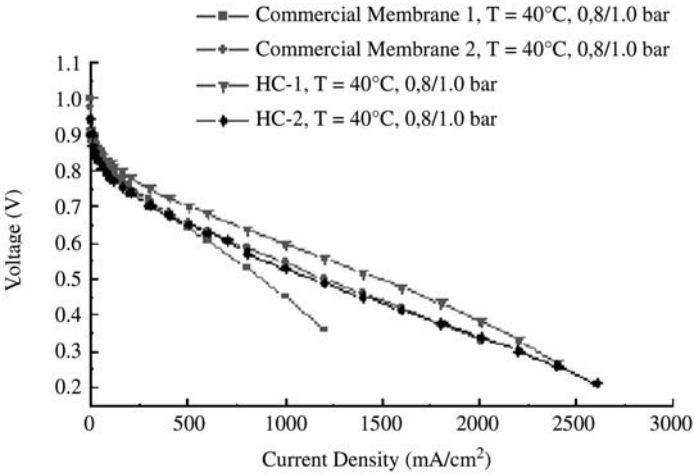

Fig. 9 Membrane performance of a single fuel cell (area: 5 cm^2, Pt loading on anode/cathode: 0.4 mg/cm^2) using commercial membranes 1 and 2, and microemulsion-synthesized membranes HC-1 and HC-2

3.2
Polymer Nanocomposites Produced by Bicontinuous-Microemulsion Polymerizations

3.2.1
Ruthenium (II) Complexes in Polymerized Bicontinuous-Microemulsions

Bicontinuous microemulsions consisting of cationic surfactant AUTMAB (30–40 wt%), MMA (30–40 wt%), and 20–40 wt% of an aqueous 50 µM solution of water-soluble metal complexes such as $Ru(dip)_3Cl_2$ (dip=4,7-diphenyl-1,10-phenanthroline) have been investigated [98]. After polymerization, the microemulsion transformed into a transparent polymer film which showed a remarkable enhancement in luminescence intensity. The emission lifetime also

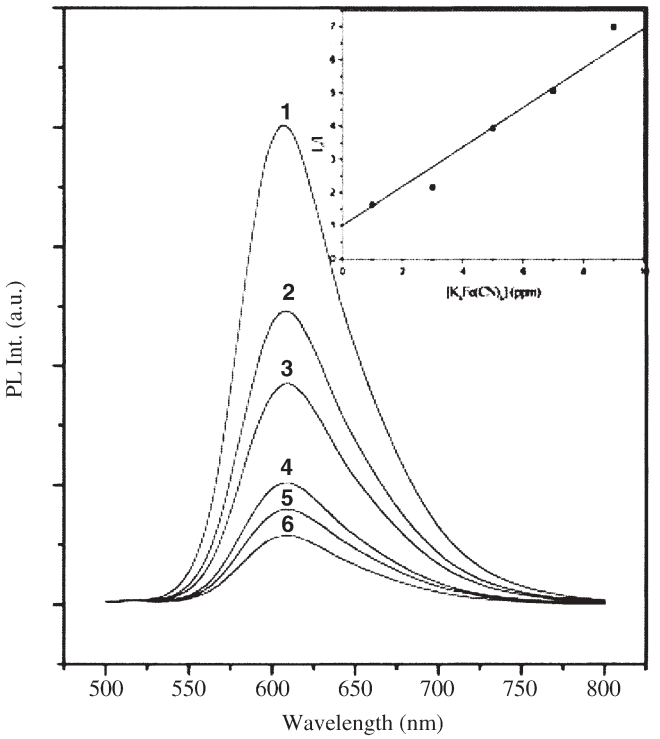

Fig. 10 The effect of potassium ferrocyanide on the luminescence spectra of $[Ru(dip)_3]^{2+}$ in polymerized cationic microemulsion: (1) 0 ppm, (2) 1 ppm, (3) 3 ppm, (4) 5 ppm, (5) 7 ppm and (6) 9 ppm. The contact time between the potassium ferrocyanide solution and the polymer film was 10 min. The insert is the Stern-Volmer plot for the quenching of $[Ru(dip)_3]^{2+}$ by potassium ferrocyanide

increased substantially from 0.98 μs (aqueous), to 2.0 μs (fluid microemulsion), to 5.8 μs for the polymerized microemulsion. The substantial increases in emission intensity and lifetime of $[Ru(dip)_3]^{2+}$ are ascribed to rigidochromism resulting from the transformation of the dynamic nanostructure of the fluid microemulsion into its solidified state after polymerization. In addition, the fluorescence of $[Ru(dip)_3]^{2+}$ could largely be quenched within 5–10 min by immersing the polymer film in a dilute (several ppm) aqueous solution of potassium ferrocyanide, as demonstrated in Fig. 10. This was possible because the polymer film possessed nanoporous open structures which enabled water and $[Fe(CN)_6]^{4-}$ ions to freely and rapidly pass through the nanochannels of the polymer network. The use of the polymerized bicontinuous microemulsion as a matrix allowed $[Ru(dip)_3]^{2+}$ complexes to be immobilized, resulting in its high sensitivity and fast response to the quencher from the external phase. This novel approach can be further developed for sensors and nanocomposites with specific functionality.

3.2.2
Aligned Nanocomposites of Ferrite-Polymer from Bicontinuous-Microemulsion Polymerization

It has been reported [99] that flame spraying of microemulsions containing nanoparticles can lead to the deposition of thin films. This is an alternative method to laser-assisted ablation and other thermal methods to evaporate metallic substrates and condense the vapors onto thin film. A novel strategy has recently been employed in the assembly of magnetic nanoparticles in polymer-nanoparticle composites using an external magnetic field [100]. A new type of hybrid colloidal assembly, combining a bicontinuous microemulsion matrix with a suspension of colloidal magnetic particles (ferrofluid), was investigated in the study. One distinct feature of this system is that the polymer matrix consists of numerous randomly interconnected channels that allow solid magnetic nanoparticles to be incorporated after the structure of the bicontinuous microemulsion matrix has been locked into place by polymerization.

The precursor, magnetic nickel ferrite nanoparticles, was prepared from mixing two W/O microemulsions, one of which contained Ni-Fe nitrate solution and the other containing ammonium hydroxide. The nickel-iron hydroxide particles formed were recovered by centrifugion followed by calcining at 500 °C for 5 h, giving the complete conversion of the hydroxide particles into magnetic nickel ferrite ($NiFe_2O_4$). The ferrofluid was then prepared by dispersing the ferrite particles in the aqueous solution stabilized by PEO-macromonomer surfactant (C_1-PEO-C_{11}-MA-40). The ferrite-microemulsion, consisting of about 33 w% water, 1–2 wt% of $NiFe_2O_4$, 35 wt% of C_1-PEO-C_{11}-MA-40, 21 wt% acrylonitrile (AN) and 9 wt% MMA was polymerized by redox initiation in a glass cell at room temperature. The transparent solid sample was microtoned to thin film, for TEM observation as shown in Fig. 11.

In the absence of a magnetic field during the polymerization, the nanoparticles of $NiFe_2O_4$ were randomly distributed in the polymerized microemulsion sample, as shown in Fig. 11a. However, under a magnetic field of a particular field strength, $NiFe_2O_4$ particles in the aqueous channels of the microemulsion could be aligned with the field without causing much agglomeration of the magnetic particles. As the polymerization of microemulsion advanced to the solidified state, the magnetic particles were locked within the water channels of the polymerized matrix along the direction of the magnetic field, as revealed by Fig. 11b. By further refining the polymerization method, magnetic particles may be patterned in polymer substrate by careful control of the external magnetic field. Many other magnetic/polymer nanocomposites can be prepared in a similar way.

This bicontinuous-microemulsion polymerization method can also be used to synthesize polymer nanocomposites containing SiO_2 [101], TiO_2, ZnO and many other semiconductors. The advantage of this method is that the nanoparticles of inorganic materials can be dispersed in the polymer matrix fairly uniformly. The only requirement is that nanomaterials should be first stabilized

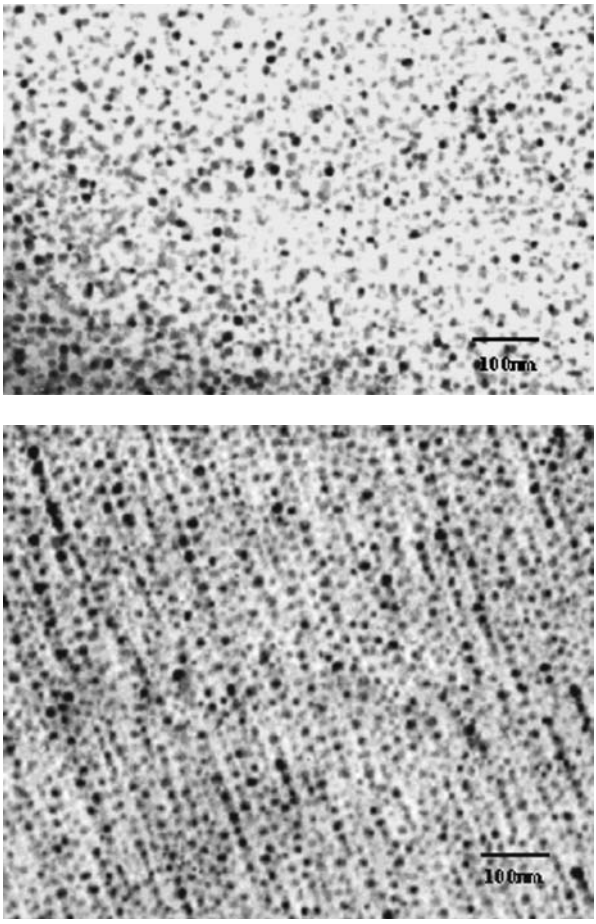

Fig. 11 TEM micrographs of polymerized ferrite-microemulsion nanocomposites containing 2 wt% $NiFe_2O_4$. **a** No magnetic field during polymerization; **b** under the influence of H=50 Oe field during polymerization

in an aqueous phase of microemulsions without causing phase separation during polymerization. Hybrid inorganic polymer materials can also be prepared from ternary microemulsions [102].

3.3 Synthesis of Nanocomposites Via In-Situ Microemulsion Polymerization

Some non-oxide nanoparticles such as PbS and CdS can be used to prepare polymer-inorganic nanocomposites by a double-microemulsion process [103]. In this case, two precursor microemulsions must be prepared separately first and then mixed together for polymerization. Using CdS-polymer nanocom-

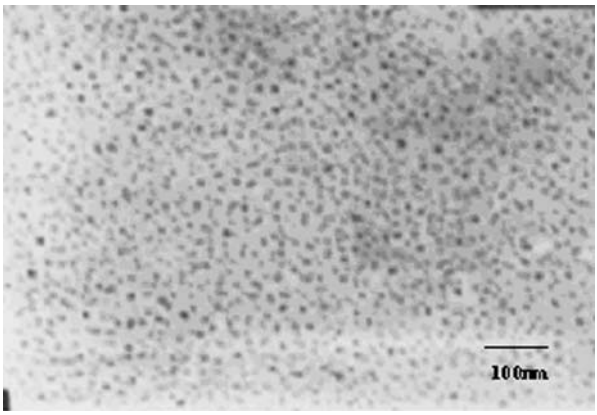

Fig. 12 TEM micrograph of Au-polymer nanocomposite prepared via in situ microemulsion polymerization

posite as an example, common compositions of two precursor microemulsions were 35 wt% MMA and 35 wt% AUDMAA. One of the microemulsions contained 30 wt% of 10 mM $CdBr_2$ aqueous solution, while the other contained 30 wt% of 10 mM $(NH_4)_2S$ aqueous solution. Two precursor microemulsions were then mixed for polymerization at 55 °C using AIBN initiator.

A dispersion of nanoparticles of Au or other metals in a polymer matrix may also be obtained by a one-pot process of microemulsion polymerization. For instance, the UV-polymerization of a microemulsion of 35 wt% MMA, 35 wt% AUDMAA and 30 wt% of 0.1 M $HAuCl_4$ aqueous solution would produce a Au-polymer nanocomposite, as shown in Fig. 12 [104]. This TEM micrograph shows a microtoned thin film of the sample. It is clearly apparent that Au particles of about 10–15 nm are well dispersed in the polymer matrix.

4
Microemulsion Reactions for Processing Inorganic Nanomaterials

The existence of microdomains or droplets with large interfacial area per unit volume in inverse and bicontinuous microemulsions opens up possibilities for controlling the inorganic reaction rates, the pathways, the stereochemistry, and the morphology of the products. By employing microemulsions, monodisperse particles of a few nanometers in diameter can be prepared for the study of quantum size effects. Many new and unusual physical and chemical properties also arise as particles attain nano-sized dimensions [105–107]. There is increasing recognition that aqueous synthesis offers growth control capabilities that can be conveniently exploited to prepare these desirable fine particles [107, 108]. The dependence of the size and polydispersity of the particles obtained on the size and concentration of the microemulsion droplets, the concentration

of the dispersed reactants, the exchange rate between the droplets, and the reactions and interactions between surfactants and metal ions or particles has already been partly addressed [109–114].

Compared to conventional solid-state reaction methods, solution-based synthesis results in higher levels of chemical homogeneity. In solution systems, mixing of the starting materials is achieved at the molecular level, and this is especially important when multi-component oxides are being prepared. As a solution-based materials synthesis technique, the microemulsion-mediated method offers a unique ability to affect particle synthesis and particle stabilization in one step. A wide variety of nanosize metal oxides – binary oxides from alumina to zirconia, as well as complex metal oxides – can be prepared by exploiting the ability of microemulsions to solubilize, compartmentalize, and concentrate reactants and products. Most of the focus in the past has been on the successful synthesis of specific metal oxide compounds as nanoparticles. Water-in-oil microemulsions (inverse microemulsions) have been the most widely used for the preparation of spherical nanoscale particles. Reagents dissolved in the water domains of an inverse microemulsion can react via intermicellar communication through dynamic collision processes. Nucleation and growth occur as the process proceeds.

Many potential applications of microemulsion-derived materials appear in the literature. The list includes catalysts, nanoporous membranes, nanocomposites and precursor powders for functional ceramics [115–139]. However, before microemulsion-derived materials become more than laboratory curiosities, two key issues must be addressed: product recovery and yield. Materials generated in microemulsion media can be used in two ways: as prepared in the fluid phase, or as recovered solids. A common practice found in the literature involves phase destabilization of microemulsions via the addition of polar solvents such as ethanol and acetone to precipitate the products. This approach works well as a laboratory technique that permits particles to be recovered for later characterization. However, it is unlikely to be an economically viable approach for practical processing, as we eventually need to separate the added solvents in order to reformulate the original microemulsion. The susceptibility of microemulsion to destabilization by electrolytes severely limits the highest concentrations that can be used for precipitation reactions. This has an adverse impact on prospects for large-scale microemulsion processing. The feasibility of microemulsion-derived synthesis depends on the availability of surfactant/oil/water formulations that give stable microemulsions during reaction, but not during precipitation reactions. Therefore, investigations that emphasize the effects of reactants and products on the stability domains of microemulsions will play an important role. Hopefully, such investigations will lead to guidelines for formulating microemulsion compositions that are compatible with large-scale material synthesis.

4.1 Synthesis of Inorganic Nanoparticles in Inverse Microemulsion

For reactions in inverse microemulsions that involve the total confinement of the reactant species within the dispersed water droplets, the exchange of reactants by the coalescence of the two droplets take place prior to their chemical reaction. The chemical reaction produces an (almost) insoluble product. The reaction medium is first saturated with this product. When the saturation exceeds a critical limit, nucleation occurs. Then the nuclei start to grow rapidly and consume the reaction product leading to a decline in the supersaturation. As soon as the supersaturation falls below the critical level, no further nucleation occurs, so only the existing particles grow beyond this point. If the time period of nucleation is short in comparision to the growth period, rather monodisperse particles are obtained.

Conceptually, these particle synthesis methods can be classified into three main groups:

1. Double inverse microemulsion
2. Inverse microemulsion plus trigger
3. Inverse microemulsion plus a second reactant, as illustrated in Fig. 13

It is apparent that a number of chemical reactions involving aqueous, organic and/or amphiphilic reagents may be accommodated in micellar systems through some of these methods or a combination of them. It is important to note that, in these processes, the reverse micelles not only serve as a passive host, but also provide hydrophobic and electrostatic interactions between the micelles. The reagents used have a profound influence on the chemical and physical properties of the resulting particles.

For the double inverse microemulsion technique, we use two separate microemulsions: reactant A solubilized in a specific microemulsion composition, and reactant B solubilized in another specific microemulsion composition. When the two microemulsions are mixed, reactants A and B will then mix within the microemulsion droplets, preventing sudden precipitation of the product AB. If reactants A and B were to be pre-mixed without using the double microemulsion technique, it would be difficult to control the particle sizes and to prevent agglomeration of particles. This is one of the principles used to produce nanoparticles with double inverse microemulsions (Fig. 13a). On the other hand, nanoparticles can also be produced in inverse microemulsions by adding a trigger (such as heat/light or a reducing/precipitating agent) to an inverse microemulsion containing the primary reactant dissolved in the aqueous core (Fig. 13b). Figure 13c shows oxide, hydroxide or carbonate precipitates formed by passing gases such as oxygen, ammonia or carbon dioxide through an inverse microemulsion containing soluble salts of the cations.

Since numerous papers have been published on the preparation of inorganic nanomaterials by microemulsions, we do not intend to review all of them here. As examples, we will describe how inverse microemulsions can be used to pre-

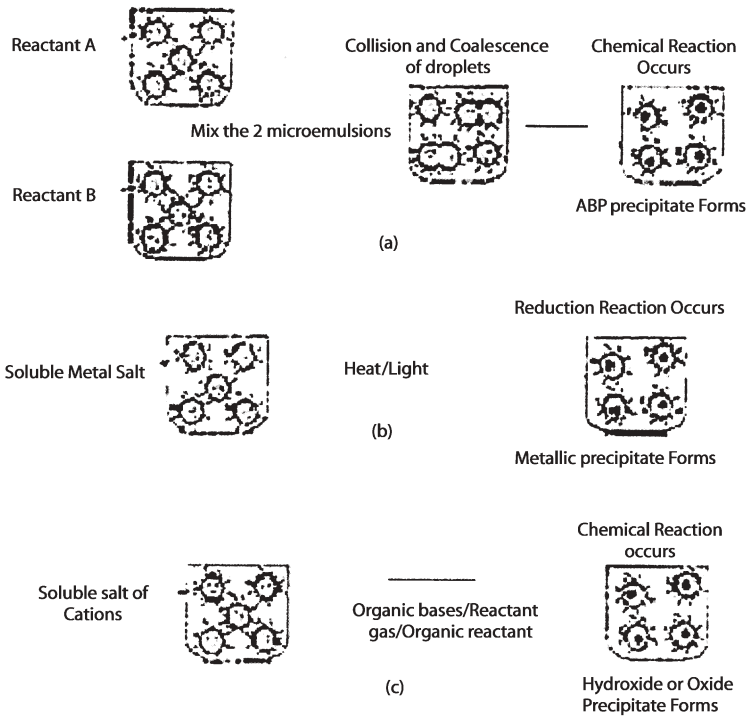

Fig. 13 Synthesis of nanoparticles in microemulsions using: **a** double inverse microemulsions; **b** inverse microemulsion plus a trigger; **c** inverse microemulsion plus reactant [122]

Table 2 Inorganic materials synthesized using inverse microemulsion

Material	Inverse microemulsion (surfactant-oil)	Investigation/results	Reference
CdS	NP-5+NP-9 and petroleum ether	To study the synthesis of CdS using hydrothermal microemulsion	[141]
PbS-coated CdS	NP-5 and petroleum ether	To study the kinetic growth and nonlinear optical response of PbS-coated CdS particles	[142]
Mn-doped ZnS	NP-5+NP-9 and	To compare the properties of Mn-ZnS particles prepared via a conventional reaction, a conventional reaction with hydrothermal treatment, a microemulsion, and a microemulsion with hydrothermal treatment	[143]

Table 2 (continued)

Material	Inverse microemulsion (surfactant-oil)	Investigation/results	Reference
$NiFe_2O_4$	NP5+NP-9 and cyclohexane	To study and characterize $NiFe_2O_4$	[144]
$BaFe_{12}O_{19}$	NP-5+NP-9 and cyclohexane	Ultrafine, high coercivity $BaFe_{12}O_{19}$ was prepared via inverse micro-emulsion and compared to that prepared using the conventional method	[145]
SiO_2	NP-5+NP-9 and cyclohexane	Influence of pH and concentration of sodium orthosilicate on the silica particle size, morphology and specific surface area	[153]
Cu-doped SiO_2	AOT+SDS and cyclohexane	To prepare and characterize Cu-SiO_2 particles	[134]
Ru-Cu-doped SiO_2	AOT+SDS and cyclohexane	The bimetallic Ru-Cu oxides supported on silica showed high catalytic conversion of N_2O	[135]
Perovskite powders	NP-5 and octane or petroleum ether	To prepare and characterize perovskites	[155]
Zirconia and zirconate	NP-5+NP-9 and cyclohexane	To produce zirconia, lead zirconate and lead zirconate titanate at much lower calcination temperatures	[158–161]
Hydroxyapetite (HA)	NP-5+NP-9 and cyclohexane	To compare differences in the sizes, morphologies and specific surface areas of HA powder prepared by W/O microemulsion, bicontinuous microemulsion and the emulsion method	[162]
Hydroxyapetite (HA)	KB6ZA and petroleum ether	To synthesize HA powders in O/W emulsion using the nonionic surfactant KB6ZA	[163]
Pt-Ru	NP-5+NP-9 and cyclohexane	To synthesize and characterize Pt-Ru catalyst for fuel cell applications	[164]

pare semiconductors, nano-sized oxide particles, and hydroxapetite nanoparticles, as illustrated in Table 2. The attraction of using nonionic polyoxyethylated alkyphenyl ether surfactants (like NP-5, NP-9, or mixture of NP-5/NP-9) is that it allow us to formulate inverse microemulsions without the need for cosurfactant; no undesirable counterions are needed. In addition, the various sizes of the hydrophilic (oxyethylene) groups or/and the hydrophobic (alkyl) groups provide flexibility during the selection of surfactant.

4.2 Materials Systems

4.2.1 Doped and Un-Doped CdS/ZnS Nanoparticles

Semiconductor nanoparticles have been extensively studied in recent years owing to their strongly size-dependent optical properties. Among these nanomaterials, CdS and PbS are particularly attractive due to their nonlinear optical behavior and unusual fluorescence or photoluminescence properties [136, 137]. A number of studies have been published recently regarding the preparation of CdS, PbS and ZnS nanoparticles in inverse microemulsion systems [138–143]. In these works, NP-5/NP-9 was the most commonly used surfactant and petroleum ether the most commonly used oil. The aqueous phase for each inverse microemulsion consisted of cadmium nitrate (0.1 M) and ammonia sulfide (0.1 M) respectively. CdS was recovered from the mixture of double microemulsions [141]. Electron microscopy revealed that the spherical particles were around 10–20 nm in diameter, as seen in Fig. 14.

The synthesis of PbS-coated CdS was conducted in a microemulsion system similar to that mentioned above, except that a third inverse microemulsion,

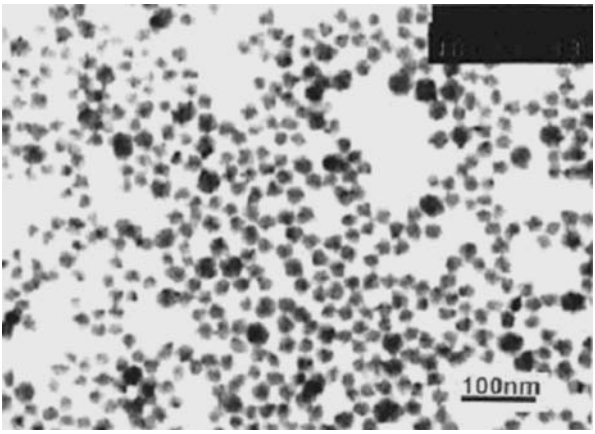

Fig. 14 Transmission electron micrograph (TEM) of a CdS cluster synthesized at 30 °C [141]

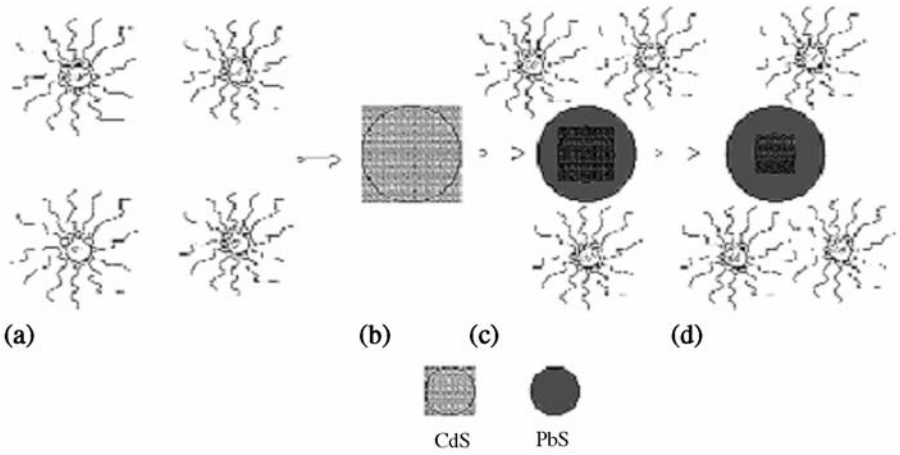

Fig. 15 Formation of PbS-coated CdS nanocomposite in microemulsion: **a** mixing of a microemulsion containing $Cd(NO_3)_2$ aqueous solution with a microemulsion containing $(NH_4)_2S$ aqueous solution; **b** formation of CdS nanoparticle in microemulsion; **c,d** Pb^{2+} ions in a third microemulsion replace the Cd^{2+} in the Cd-S band and diffuse through the PbS layer to form the PbS shell [142]

containing lead nitrate (0.1 M) in the aqueous phase, was also needed [142]. This is to encourage the formation of PbS shells around the CdS particle cores, as depicted Fig. 15. Pb^{2+} ions displaced some Cd^{2+} in the Cd–S bonds to form Pb–S bonds on the surfaces of the CdS particles. The thicknesses of the PbS shells in the PbS-coated nanocomposite could be controlled by changing the Pb^{2+} ion concentration. Absorption measurements of the mixed systems as a function of the concentration of lead nitrate solution indicated a continuous trend toward the PbS spectrum with increasing Pb^{2+} concentration. The particle sizes of the CdS, PbS and CdS/PbS composites are shown in Fig. 16. The resulting NLO properties of the CdS and PbS and CdS/PbS nanocomposite particles were determined by a femtosecond Z-scan technique. A large refractive nonlinearity in these nanocomposite particles was observed due to the optical Stark Effect and strong interfacial and inter-particle interactions. These nanoparticles with large refractive nonlinearities may find application in optical devices, such as those for optical limiting and switching.

Mn-doped ZnS powders were also prepared by inverse microemulsion under hydrothermal treatment at 120 °C [143]. This produced ultrafine and agglomerate-free particles 5–20 nm in diameter. In contrast, the particles prepared via conventional aqueous solutions often coagulated, forming large aggregated clusters. Furthermore, compared with Mn-doped ZnS materials synthesized through conventional aqueous reactions, the nanoparticles prepared in microemulsion showed significantly enhanced photoluminescence. In particular, the photoluminescence of particles prepared in microemulsion under hydrothermal treatment was found to be 60 times higher than that for material

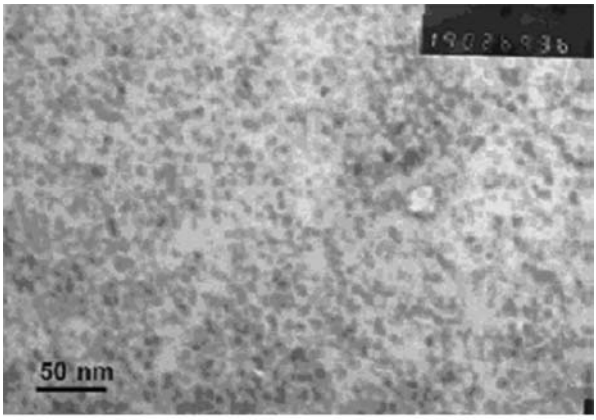

(a)

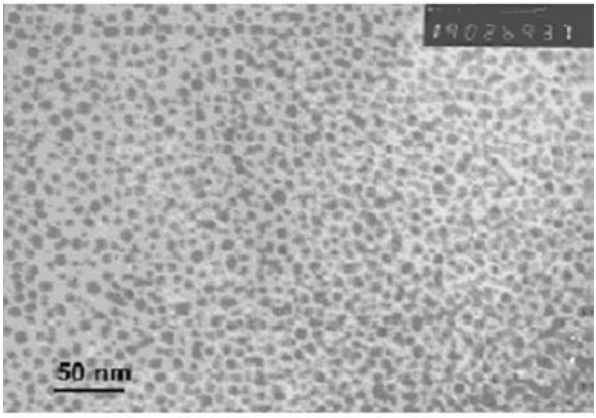

(b)

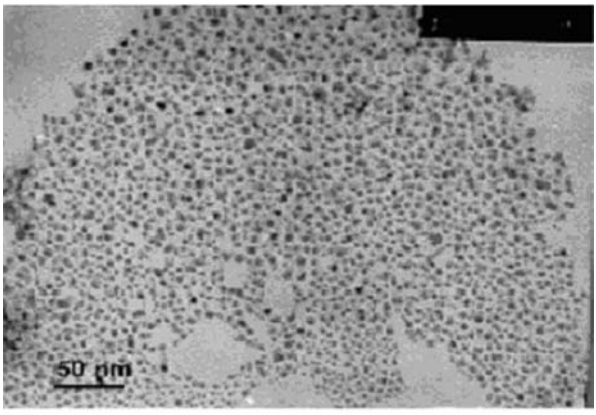

(c)

Fig. 16 Transmission electron micrographs of **a** CdS, **b** PbS nanoparticles, and **c** PbS-coated CdS nanocomposite [142]

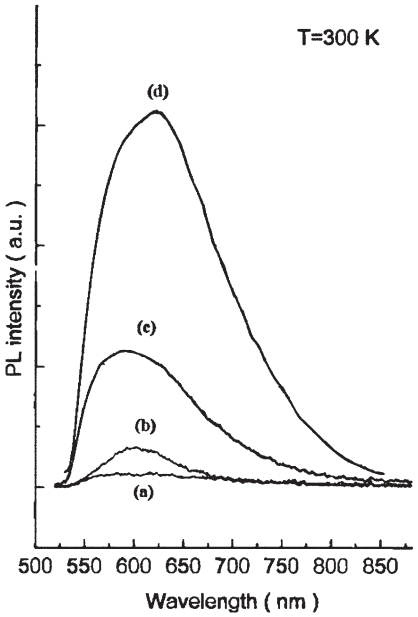

Fig. 17 Photoluminescence (PL) of ZnS:Mn^{2+} particles prepared by: **a** conventional reaction at room temperature; **b** conventional reaction with hydrothermal treatment; **c** microemulsion at room temperature; **d** microemulsion with hydrothermal treatment, with an excitation intensity of 4 W/cm^2 [143]

obtained through the direct aqueous reaction at room temperature (as shown in Fig. 17). This dramatic increase in photoluminescence yield is attributed to the surface passivation of nanoparticles by the adsorption of surfactants, the formation of sphelerite with cubic zinc blende structure, and Mn migration into the interior lattice of the ZnS host.

4.2.2 Magnetic Ferrites

Nano-sized magnetic ferrite particles are the subject of intensive research because their physical properties are quite different from those of the bulk material. The magnetic characteristics of particles used for recording media crucially depend on their sizes and shapes. So, the material used for high-quality recording media should be ultrafine, chemically homogeneous, and stable, with a narrow particle size distribution a predetermined shape. These requirements demand a reliable and reproducible preparation technique.

The formation of microhomogeneous nanoparticles of nickel and barium ferrite was carried out in a three-component microemulsion consisting of NP-5/NP-9 as the surfactant, cyclohexane as the oil, and an aqueous solution of

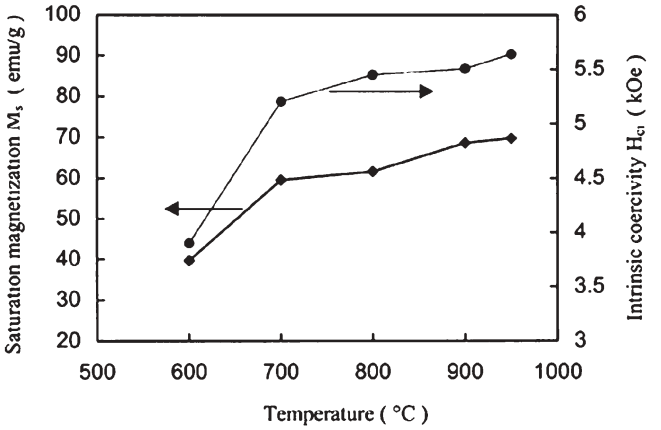

Fig. 18 The saturation magnetization and intrinsic coercivity as a function of calcination temperature for the microemulsion-derived barium ferrites [145]

nickel nitrate and ferric nitrate [144]. An immediate precipitation was affected by adding ammonia to the microemulsion, and the resulting amorphous precipitate was transformed into nickel ferrites by calcining at 600 °C. Discrete nickel ferrite particles with polyhedron shapes and an average size range from 10–20 nm were obtained. The sol-particles were identified as $NiFe_2O_4$ by Mossbauer spectroscopy, electron diffraction and X-ray spectroscopy. Magnetic measurement revealed a saturation magnetization value of 43.0 emu/g for the sample calcined at 500 °C.

Barium ferrite particles were obtained by mixing a ferric ion-containing microemulsion and a barium-containing microemulsion [145]. Precipitation of the hydroxide precursor was affected by adding ammonia solution dropwise into the microemulsions under stirring. The resulting barium ferrite particles formed at a calcination temperature of 950 °C. The round particles synthesized were well dispersed, although a limited degree of particle agglomeration was also observed. The average size of the calcined particles was in the range of 100–200 nm, which was about ten times bigger than the average size of the precursor particles. A high saturation magnetization of 69.74 emu/g and an intrinsic coercivity of 5639 Oe were obtained for the powder calcined at 950 °C (Fig. 18). These results are comparable to some of the best ever reported for fine barium ferrite powders prepared via chemistry-based processing routes. The much improved saturation magnetization and coercivity can be explained by the high phase purity and well-defined crystallinity of $BaFe_{12}O_{19}$ developed in the microemulsion-derived precursor when calcined at a temperature that is high enough.

4.2.3 Silica and Silica-Supported Ru-Cu Oxides

The vast majority of techniques published for the microemulsion-mediated synthesis of silica [146–151] are based on the alkoxide sol-gel method. The oil-soluble metal alkoxide was added to a microemulsion containing solubilized water. The alkoxide must diffuse through the oil continuous phase to the water pool where the hydrolysis and condensation reactions take place.

In our studies, the nano-sized silica was synthesized using cheap sodium orthosilicate and sodium metasilicate rather than expensive alkoxysilanes. An inverse microemulsion containing NP-5/NP-9 as surfactant and cylcohexane or petroleum ether as the oil was used to carry out the hydrolysis and condensation of sodium orthosilicate or metasilicate using an acidic medium [152, 153]. The spherical silica particles of size 10–20 nm were obtained in a system using cyclohexane as the oil and with sodium orthosilicate of 0.01–0.1 M [152]. The particle size increased as the concentration of sodium orthosilicate and the pH were increased. Silica particles prepared in basic conditions were more uniform in size than those prepared in an acidic medium. But calcined silica powders with larger specific areas (350–400 m^2/g) were obtained for those prepared in an acidic medium.

Much smaller silica particles of about 5–10 nm were formed by the controlled hydrolysis and polymerization of sodium metasilicate in bicontinuous microemulsions [153]. The bicontinuous microemulsion system consisted of NP-5/NP-9, petroleum ether, and a high concentration of sodium metasilicate solution (0.2 M). This example illustrates the feasibility of using bicontinuous microemulsion to synthesize silica powders with high specific surface areas (~400 m^2/g) and good amorphous stabilities at 600 °C. The treatment of some calcined silica powders with hexadecyltrimethylammonium hydroxide increased their specific surface areas still further, from 350 to 510 m^2/g.

The double microemulsion-mediated process also provides a convenient method for preparing a metal-containing silicate coating. The two microemulsion systems contained two common components: anionic surfactant AOT and cyclohexane [134]. The difference was that the first microemulsion consisted of an aqueous solution of sodium metasilicate (0.2 M) and 10 wt% SDS as the co-surfactant, while the second microemulsion consisted of an aqueous solution of copper nitrate (0.1 M) and 10 wt% SDS. The copper-ion microemulsion was added to the silicate-ion microemulsion with constant stirring. After 8 h of gellation, and ageing for an additional 24 h, copper nitrate crystals were identified within the silicate network. Silica-copper composite powders with various copper contents (4–20 wt%) and surface areas of 200–400 m^2/g were synthesized.

Using a variation on the microemulsion-mediated process, catalytic bimetallic Ru-Cu oxides supported by silica were made through the controlled hydrolysis/polymerization of sodium metasilicate, copper nitrate and ruthenium chloride via a single microemulsion protocol [135]. With AOT and SDS-based microemulsion, a high specific surface area (~400 m^2/g) and uniform pore size

(~38 Å) of the produced catalyst can be maintained during catalytic reactions. Moreover, tests of the catalytic activity indicated a high catalytic conversion of N_2O by the catalysts synthesized from the microemulsion process at a lower temperature (~400 °C) than that prepared from traditional impregnation processes. The uniform elemental distribution of RuO_2 on the SiO_2 produced by this microemulsion process was established by XPS and SEM/line scanning.

4.2.4 Perovskites

The complex oxides that belong to the group known as perovskites have the general formula ABO_3, where the ionic charges on the metals can assume the form $A^+B^{5+}O_3$, $A^{2+}B^{4+}O_3$ and $A^{3+}B^{3+}O_3$. The first microemulsion-mediated process to synthesize a perovskite used a double microemulsion protocol based on a nonionic surfactant Genapol OX/decane/water system [154]. A microemulsion containing $BaCl_2$ and $TiCl_4$ in the dispersed phase was mixed with an oxalic acid-containing microemulsion. However, X-ray diffraction could not confirm the presence of the intermediate barium titanyl oxalate and the calcined solid did not yield barium titanate.

The double inverse microemulsion method was also used to synthesize perovskite-type mixed metal oxides [155]. One microemulsion solution contained nitrate salts of either $Ba(NO_3)_2/Pb(NO_3)_2$, $La(NO_3)_3/Cu(NO_3)_2$ or $La(NO_3)_3/Ni(NO_3)_2$, and the other microemulsion contained ammonium oxalate or oxalic acid as the precipitant. These metal oxalate particles of about 20 nm were readily calcined into single phase perovskite-type $BaPbO_3$, La_2CuO_4 and $LaNiO_3$. The calcinations required for the microemulsion-derived mixed oxalates were 100–250 °C below the temperatures used for the metal oxalates prepared by a conventional aqueous solution precipitation method.

4.2.5 Zirconia, Lead Zirconate and Lead Zirconate Titanate

Most zirconia nanoparticles have been prepared by the microemulsion-mediated alkoxide sol-gel method [156, 157] using zirconium tetrabutoxide as the alkoxide precursor. The first step is to synthesize zirconium hydroxide precursor particles via double inverse microemulsions and then they are calcined to zirconia [158]. Three types of processing routes have been used to prepare fine lead zirconate ($PbZrO_3$) powders: a conventional solid reaction, conventional coprecipitation using either oxalic acid or ammonia solution as the precipitant, and microemulsion-refined coprecipitation using either oxalic acid or ammonia solution. The microemulsion-derived precursors exhibited a much lower formation temperature for the orthorhombic $PbZrO_3$ phase [159] than that of the conventionally coprecipitating precursors. Ammonia solution appeared to be a better precipitant than oxalic acid for reducing the formation temperature of $PbZrO_3$. It was concluded that microemulsion-derived $PbZrO_3$

powders were much finer and has less particle-particle agglomeration. The synthesis of $PbZrO_3$ powders could also be performed via a polyaniline-mediated microemulsion process [160]. A small amount (~4 wt%) of polyaniline was retained in the microemulsion-derived oxalate precursor by an in situ polymerization of lead oxalate and zirconate oxalate. The in situ polymerization of aniline on the surfaces of the oxalate particles resulted in the formation of a well-dispersed precursor powder. Upon calcination at 800 °C, ultrafine lead zirconate powder was obtained.

Low temperature synthesis of lead zirconate titanate (PZT) can also be obtained via a microemulsion process [161]. The microemulsion, containing cations of lead zirconium and titanium in the aqueous phase, was coprecipitated as hydroxide precursors by the addition of ammonium solution. Crystalline tetragonal PZT powders were then obtained by calcining the precursors at a temperature as low as 450 °C in air without forming any intermediate phases.

4.2.6 Hydroxyapetite (HA)

Hydroxyapetite ($Ca_{10}(PO_4)_6(OH)_2$) is the major constituent of human bone and teeth. The strength of HA in almost all of its applications is largely determined by its specific surface area, and so a nanocrystalline HA powder is required.

Ultrafine HA powders can be produced by reacting $CaCl_2$ and $(NH_4)_2HPO_4$ in bicontinuous microemulsion, W/O microemulsion and emulsion, which have the same basic components of cyclohexane, nonionic surfactant (NP-5/NP-9) and aqueous solution [162]. HA powder particle size, chemical homogeneity, and the degree of particle agglomeration all depend on the reaction medium. Both bicontinuous and W/O microemulsions lead to the formation of much finer HA powders than those prepared from the emulsion composition. This is because the precipitates formed in both bicontinuous and W/O microemulsions are limited in size by the dimensions of the nano-sized reaction domains. In contrast, the aqueous droplets in the emulsion are much bigger, and therefore the HA particles obtained are twice as large as those formed in nano-sized domains. It was found that the specific surface area of the powder prepared by bicontinuous microemulsion was 86.03 m^2/g, 76.64 m^2/g by W/O microemulsion, and 42.63 m^2/g by emulsion. Much smaller degrees of particle agglomeration were observed for HA powders obtained by bicontinuous and W/O microemulsions, but the powders prepared from emulsion showed a larger average agglomerate size of 1.1 μm, which was twice the size observed from the former two.

A similar study was performed on the formation of nanocrystalline HA in nonionic surfactant emulsions [163]. Instead of using NP-5/NP-9 surfactant, KB6ZA (nonionic surfactant which is a lauryl alcohol condensed with an average of 6 mol of oxyethylene oxide) was used together with petroleum ether as the oil phase to prepare HA powder in an O/W emulsion system. One of the very apparent advantages of using O/W emulsion over W/O microemulsion is

the high production yield using smaller amounts of oil and surfactant. In this study, HA was prepared by reacting $CaCl_2$ and $(NH_4)_2HPO_4$ in three reaction systems: a conventional aqueous solution, a micellar solution containing 3.2 wt% of the nonionic surfactant KB6ZA and 1.0 M $CaCl_2$ solution, and O/W emulsions containing KB6ZA with varying amounts of petroleum ether and 1.0 M $CaCl_2$ solution. For the emulsion system, the oil phase residing in the hydrophobic cores of the oil-swollen micelles lead to a large expansion in the micellar dimensions, in the form of emulsion droplets. This undoubtedly increases the reaction sites between $CaCl_2$ and $(NH_4)_2HPO_4$ at the interfaces, as shown schematically in Fig. 19. Moreover, the emulsion droplets are more stable than the surfactant micelles and the average life-span of an emulsion droplet is much longer than that of a micelle. All of these factors make an emulsion system much more suitable than a micellar system for forming HA particles of high crystallinity. The enhanced crystallinity of HA derived from the emulsion composition derives from the complexation of Ca^{2+} by oxyethylene groups of the nonionic surfactant. The resulting HA precursor powders underwent little growth in crystallite and particle sizes upon calcination at 650 °C for 6 h.

4.2.7 PtRu/C Catalysts

PtRu alloys are currently the most active anode catalysts for the oxidation of methanol or CO-contaminated H_2, (like H_2 derived from reformed methanol) in low temperature solid polymer electrolyte fuel cells such as direct methanol fuel cells (DMFC) or indirect methanol fuel cells (IMFC). High surface area catalysts are generally prepared by co-impregnation,coprecipitation, absorbing alloy colloids, or surface organometallic chemistry techniques. For both alloy and oxide promoted catalytic systems it is important that Pt and the second metal (or metal oxide) are in intimate contact. This close association of the platinum and the co-catalyst can be difficult to achieve using conventional catalyst preparation techniques because the active components may be deposited at different sites on the support surface. As the preparation details control the final composition, surface structure and morphology of the catalysts, it is not surprising to learn that catalytic activity is strongly dependent on preparation conditions.

Nano-sized PtRu catalysts supported on carbon have been synthesized from inverse microemulsions and emulsions using H_2PtCl_6 (0.025 M)/$RuCl_3$ (0.025 M)/NaOH (0.025 M) as the aqueous phase, cyclohexane as the oil phase, and NP-5 or NP-9) as the surfactant, in the presence of carbon black suspended in a mixture of cyclohexane and NP-5+NP-9 [164]. The titration of 10% HCHO aqueous solution into the inverse microemulsions and emulsions resulted in the formation of PtRu/C catalysts with average particle sizes of about 5 nm and 20 nm respectively. The RuPt particles were identified by X-ray diffraction, X-ray photoelectron, and BET techniques. All of the catalysts prepared show characteristic diffraction peaks pertaining to the Pt fcc structure. XPS analysis

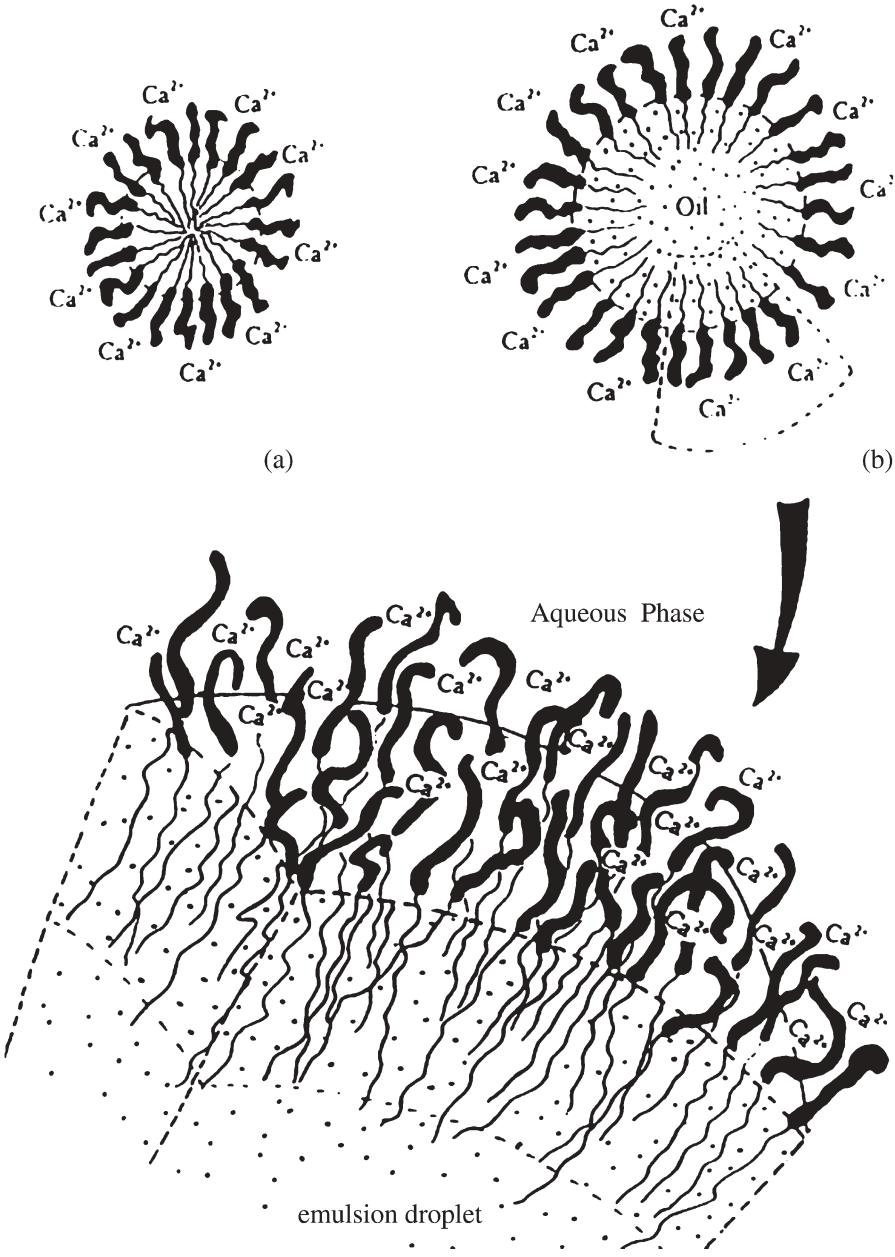

Fig. 19 Micelle and emulsion droplets in $CaCl_2$ aqueous solutions: The calcium-rich shell in the adsorbed state, at the: **a** micelle-water interface; **b** emulsion droplet surface. The surfactant molecules are represented by the zig-zag lines with Ca^{2+} heads

also revealed that the catalysts contained mostly Pt(0) and Ru(0), with a little Pt(II), Pt(IV) and Ru(IV). The double microemulsion-derived PtRu/C catalysts had higher electrocatalytic activities for methanol oxidation than that of the emulsion-derived PtRu/C electrocatalyst. The peak current density for methanol oxidation at PtRu/C obtained from the transparent inverse microemulsion was about four times higher that of the emulsion-derived PtRu/C.

4.2.8 Polymer-Coated Inorganic Nanoparticles

Nanoparticles of polyaniline/$BaSO_4$ composite, about 10–20 nm in diameter, have also been synthesized by mixing double inverse microemulsions that have some components of surfactant and oil, but different aqueous solutions [165]. The aqueous solution of one microemulsion should contain $BaCl_2$ and aniline, while the other contains $K_2S_2O_8$ and H_2SO_4. After mixing both microemulsions, nanoparticles of $BaSO_4$ are formed instantaneously with the subsequent polymerization of aniline on the surface of $BaSO_4$ particles, as verified by Rutherford backscattering measurements. The conductivity of the polyaniline/$BaSO_4$ nanocomposites increased almost linearly from 0.017 to 5 S/cm withincreasing polyaniline content in the composites (which was varied from 5 to 22 wt%). This result shows that a selection of double inverse microemulsion reactions for producing some nanocomposites of polymer/inorganic materials can be conveniently carried out by a single-step microemulsion process.

5 Conclusions

The synthesis of polymer nanomaterials by microemulsion processes is reaching maturity. Microlatexes of both hydrophilic and hydrophobic polymers can now be produced by semi-continuous microemulsion processes yielding high weight ratios of polymer to surfactant at a level attractive for to industry. However, the W/O microemulsion processes capable of producing inorganic nanomaterials with unique properties are not ready for large-scale production, because large amounts of surfactant are still needed. Bicontinuous microemulsion processes should be explored for inorganic nanomaterial production since they require lower amounts of surfactant and give higher yields.

The recent development of using polymerizable surfactants in microemulsion polymerizations has enabled the production of transparent solid polymers with some nanostructure. Randomly distributed bicontinuous nanostructures of water channels and polymer domains in solid polymers can be readily obtained from the polymerization of bicontinuous microemulsions consisting of various types of vinyl monomers and polymerizable surfactants with no allylic hydrogen.

These transparent polymers with inherent bicontinuous nanostructures may be suitable for nanofiltration, selective permeable membranes for sepa-

ration, or proton exchange membranes for fuel cell applications. The surface characteristics of the nanostructured membranes can be modified further using suitable functional monomers. New polymerizable microemulsion systems will be devised for specific copolymers and inorganic/polymer nanocomposites. Some tailor-made nanostructure polymeric materials may therefore be obtained by the polymerizable bicontinuous-microemulsion approach.

References

1. Zana R, Lang J (1987) In: Frieberg SE, Bothorel (eds) Microemulsions: structure and dynamics. CRC, Boca Raton, FL, Ch 6
2. Biasia J, Clin B, Laolanne P (1987) In: Friberg SE, Bothorel P (eds) Microemulsions: structure and dynamics. CRC, Boca Raton, FL, Ch 1
3. Frieberg SE, Bothorol P (1986) In: Friberg SE, Bothorel P (eds) Microemulsions: structure and dynamics. CRC, Boca Raton, FL
4. Winsor PA (1948) T Faraday Soc 44:376
5. Candau F (1999) In: Kumar P, Mittal KL (eds) Handbook of microemulsion science and technology. Marcel Dekker, New York, Ch 22, p 679
6. Gan LM, Chew CH (2001) In: Nalwa HS (ed) Advanced functional molecules and polymers. Gordon and Breach, New York, Ch 2, p 35
7. (a) Lopez-Quintela MA, Rivas J (1993) J Colloid Interf Sci 158:446; (b) Aikawa K, Kaneko K, Tamura T, Fujitsu M, Ohbu K (1999) Colloids Surface A 150:95; (c) Zarur AJ, Ying JY (2000) Nature 403:65; (d) Rymes J, Ehret G, Hilaire L, Boutonnet M, Jiratova K (2002) Catal Today 75:297
8. Klier J, Tucker CJ, Kalantar TH, Green DP (2000) Adv Mater 18:1751
9. Gan LM, Chew CH (1996) In: Salamone (ed) Polymeric materials encyclopedia. CRC, Boca Raton, FL, M4321
10. Candau F (1992) In: Paleos CM (ed) Polymerization in organized media. Gordon and Breach, New York, p 215
11. Candau F (1998) In: Kumar P, Mittal KL (eds) Microemulsions: fundamental and applied aspects. Marcel Dekker, New York
12. Herrera JR, Peralta RD, Lopez RG, Cesteros LC, Puig JE (2003) Polymer 44:1795
13. Candau F, Leong YS, Pouyet G, Candau SJ (1984) J Colloid Interf Sci 101:167
14. Candau F, Yong YS, Fitch RM (1985) J Polym Sci Pol Chem 23:193
15. Candau F (1987) In: Mark H, Bikales NM, Overberger CG, Menges G (eds) Encyclopedia of polymer science and engineering. Wiley, New York, 9:718
16. Vaskova V, Juranicova V, Barton J (1990) Makromol Chem 191:717
17. Vaskova V, Hlouskova Z, Barton J, Juranicova V (1990) Makromol Chem 193:267
18. Lezovic M, Ogino K, Sato H, Capek I, Barton J (1998) Polymer Int 46:269
19. Barton J, Kawamoto S, Fujimoto K, Kawaguchi H, Capek I (2000) Polymer Int 49:358
20. Barton J, Capek I (2000) Macromolecules 33:5353
21. Candau F (1989) In: El-Nokaly M (ed) ACS Sym Ser 384, Ch 4
22. Canadu F, Anquetil JY (1998) In: Shah DO (ed) Micelles, microemulsions and monolayers. Marcel Dekker, New York, p 193
23. Candau F, Zekhnini Z, Durand JP (1987) Prog Colloid Polym Sci 73:33
24. Corpart JM, Candau F (1993) Colloid Polym Sci 271:1055
25. Corpart JM, Selb J, Candau F (1993) Polymer 34:3873
26. Candau F, Buchert P (1990) Colloids Surface 48:107
27. Candau F, Pabon M, Anqueti (1999) Colloids Surface A 153:47

28. Sosa N, Peralta RD, Lopez RG, Ramos LF, Katine I, Certeros C, Mendizabal E, Puig JE (2001) Polymer 42:6923
29. Braun O, Selb J, Candau F (2001) Polymer 42:8499
30. Candau F, Braun O, Essler F, Stahler K, Selb J (2002) Macromol Symp 179:13
31. Stoffer JO, Bone T (1980) J Disper Sci Technol 1:37
32. Atik SS, Thomas JK (1981) J Am Chem Soc 103:4279
33. Tang HI, Johnson PL, Gulari E (1984) Polymer 25:1357
34. Kuo PL, Turro NJ, Tseng CM, El-Aasser MS, Vanderhoft JW (1987) Macromolecules 20:1216
35. Feng L, Ng KY (1990) Macromolecules 23:1048
36. Gan LM, Chew CH, Lye I (1992) Makromol Chem 193:1249
37. Gan LM, Chew CH, Frieberg SE (1983) J Macromol Sci Chem A 19:739
38. Ferrick MR, Murtagh J, Thomas JK (1989) Macromolecules 22:1515
39. Antonietti M, Bremser W, Muschenborn D, Rosenaur C, Schupp B, Schmidt M (1991) Macromolecules 24:6636
40. Rodriguez-Guadarrama LA, Mendizabal E, Puig JE, Kaler EW (1993) J Appl Polym Sci 48:775
41. Gan LM, Chew CH, Ng SC, Loh SE (1993) Langmuir 9:2799
42. Gan LM, Chew CH, Lee KC, Ng SC (1993) Polymer 34:3064
43. Larpent C, Tados RF (1991) Colloid Polym Sci 269:1171
44. Full AP, Puig JE, Gron LU, Kaler EW, Minter JR, Meurey TH, Texter J (1992) Macromolecules 25:5157
45. Capek I, Potisk P (1995) Eur Polym J 31:1269
46. Capek I, Fouassier JP (1997) Eur Polym J 33:173
47. Capek I, Juranicova V (1996) J Polym Sci Pol Chem 34:575
48. Capek I, Juranicova V, Barton J, Asua JM, Ito K (1997) Polymer Int 43:1
49. Guo JS, Sudol ED, Vanderhoff JW, El-Aasser MS (1992) J Polym Sci Pol Chem 30:691
50. Puig JE, Perez-Luna VH, Macias ER, Rodriguez BE, Kaler EW (1993) Colloid Polym Sci 271:114
51. Co CC, Cotts P, Burauer S, deVries R, Kaler EW (2001) Macromolecules 34:3245
52. Kukulj D, Davis TP, Gilbert RG (1998) Macromolecules 31:994
53. Hentze HP, Kaler EW (2003) Curr Opin Coll Interf Sci 8(2):164–178
54. Mendizabal E, Flores J, Puig JE, Katime I, Lopez-Serrano F, Alvarez J (2000) Macromol Chem Phys 201:1259
55. Co CC, Kaler EW (1998) Macromolecules 31:3203
56. Morgan JD, Kaler EW (1998) Macromolecules 31:3197
57. Sanghvi PG, Pokhriyal NK, Devis (2002) J Appl Polym Sci 84:1832
58. Gan LM, Chew CH, Lee KC, Ng SC (1994) Polymer 35:2659
59. Loh SE, Gan LM, Chew CH, Ng SC (1995) J Macromol Sci Pure A32:1681
60. Gan LM, Lee KC, Chew CH, Tok ES, Ng SC (1995) J Polym Sci Pol Chem 33:1161
61. Sutterline N, Kurth HJ, Markett G (1976) Angew Makromol Chem 177:1549
62. Aguiar A, Gonzales-Villegas S, Rabelero M, Mendizabal E, Puig JE (1999) Macromolecules 32:6767
63. Jang J, Ha H (2002) Langmuir 18:5613
64. Jang J, Lee K (2002) Chem Comm 1098
65. Gan LM, Lian N, Chew CH, Li GZ (1994) Langmuir 10:2197
66. Xu XJ, Siow KS, Wong MK, Gan LM (2001) Langmuir 17:4519
67. Ming W, Jones FN, Fu SK (1998) Polym Bull 40:749
68. Ming W, Jones FN, Fu SK (1998) Macromol Chem Phys 199:1075
69. (a) Xu XJ, Chew CH, Siow KS, Wong MK, Gan LM (1999) Langmuir 15:8067; (b) Chudej J, Capek I (2002) Polymer 43:1681

70. Dan Y, Yang YH, Chen SY (2002) J Polym Sci 85:2839
71. Barrere M, Silva SC, Balic R, Ganachaud F (2002) Langmuir 18:941
72. Xu XJ, Chow PY, Quek CH, Hng HH, Gan LM (2003) J Nanosci Nanotechno 3:3
73. Xu XJ, Siow KS, Wong MK, Gan LM (2001) Colloid Polym Sci 279:879
74. Xu XJ, Siow KS, Wong MK, Gan LM (2001) J Polym Sci Polym Chem 39:1634
75. Xu XY, Chow PY, Gan LM (2001) J Nanosci Nanotechno (in press)
76. Menger FM, Tsuno T, Hammond GS (1990) J Am Chem Soc 112:1263
77. Sáenz de Buruaga A, Capek I, de la Cal JC, Asua JM (1998) J Polym Sci Pol Chem 36:737
78. Antonietti M, Basten R, Gröhn F (1994) Langmuir 10:2498
79. Puig JE, Aguiar A, González-Villegas S (1999) Macromolecules 32:6767
80. Kaler EW, Co CC, de Vries R (2001) Macromolecules 34:3224
81. Kaler EW, Co CC, de Vries R (2001) Macromolecules 34:3233
82. Palani Raj WR, Sathav M, Cheung HM (1991) Langmuir 7:2586
83. Sasthav M, Cheung HM (1991) Langmuir 7:1378
84. Strey R, Lade O, Beizai K, Sottmann T (2000) Langmuir 16:4122
85. Gan LM, Chew CH (1983) J Disper Sci Technol 4:291
86. Palani Raj WR, Sasthav M, Cheung HM (1992) Langmuir 8:1931
87. Gan LM, Li TD, Chew CH, Teo WK (1995) Langmuir 11:3316
88. Gan LM, Li TD, Chew CH, Teo WK,Gan LH (1996) Langmuir 12:5863
89. Antonietti M, Hentze HP (1996) Colloid Polym Sci 274:696
90. Gan LM,Chieng TH, Chew CH, Ng SC, Pey KL (1996) Langmuir 12:319
91. (a) Gan LM, Li TD, Chew CH, Quek CH, Gan LH (1998) Langmuir 14:6068; (b) Guyot A, Tauer K (1994) Adv Polym Sci 111:44
92. Gan LM, Chieng TH, Chew CH, Teo WK, Gan LH (1996) Langmuir 10:4022
93. Liu J, Gan LM, Chew CH, Teo WK, Gan LH (1997) Langmuir 13:6421
94. Gan LM, Chow PY, Chew CH, Ong CL, Wang J, Xu G (1999) Langmuir 15:3202
95. Xu G, Ong CL, Gan LM, Ong CK, Chan HSO (1999) J Phys Chem B 10: 7573
96. Gan LM, Xu W, Siow KS, Gao Z, Lee SY, Chow PY (1999) Langmuir 15: 4812
97. Gan LM, Chow PY, Han M, Liu ZL, Yeo E (2002) In: Proc 1st Int Conf on Materials Processing for Properties and Performance, Singapore, 1–3 August 2002
98. Moy HY, Chow PY, Yu WL, Wong KMC, Yam VWW, Gan LM (2002) Chem Comm 9:982
99. Bonini M, Bardi U, Berti D, Neto C, Baglioni P (2002) J Phys Chem B 106:6178
100. Chow PY (2002) PhD Thesis, National University of Singapore, Singapore (to be published)
101. Chow PY, Gan LM (2003) J Nanosci Nanotechno 4(1–2):197–202
102. Donescu D, Fusulan L, Petcu C, Vasilescu M, Deleann C. Udrea S (2002) Macromol Symp 179:315
103. Liu B, Li HP, Chew CH, Que WX, Lam YL, Kam CH, Gan LM, Xu GQ (2001) Mater Lett 51:461
104. Quek CH, Gan LM (work to be published)
105. Andreas RP, Averback RS, Brown WL, Brus LE, Goddard III WA, Kaldor A, Louie SG, Moskovits M, Peercy PS, Riley SJ, Siegel RW, Spaepen F, Wang Y (1989) J Mater Res 4:704
106. Ichinose N, Ozaki Y, Kashu S (1988) Superfine particle technology. Springer, Berlin Heidelberg New York
107. Haruta M, Delmon B (1986) J Chem Phys 83:859
108. Brinker CJ, Scherer GW (1990) In: Sol-gel science. Academic, New York
109. Lianos P, Thomas JK (1986) Chem Phys Lett 125:299
110. Lianos P, Thomas JK (1987) J Colloid Interf Sci 125:505
111. Barnickel P, Wokaun A, Sager W, Eicke HF (1992) J Colloid Interf Sci 148:80
112. Petit C, Jain TK, Billoudet F, Pileni MP (1994) Langmuir 10:4446

113. Pileni MP (1993) Adv Colloid Interf Sci 46:139
114. Pileni MP (2003) Nat Mater 2:145
115. Inouye K, Endo R, Otsuka Y, Miyashiro K, Kaneko K, Ishikawa T (1982) J Phys Chem 86:1465
116. Fendler JH (1987) Chem Rev 87:877
117. Matson DW, Fulton JL, Smith RD (1987) Mater Lett 6:31
118. Bandow S, Kimura K, Kon-on K, Kitahara A (1987) Jpn J Appl Phys 26:713
119. Kandori K, Shizuka N, Gobe M, Kon-on K, Kitahara A (1987) J Disper Sci Technol 8:477
120. Hou MJ, Shah DO (1988) Interfacial phenomena in biology and materials processing. Elsevier, Amsterdam, p 443
121. Nagy JB (1989) Colloids Surface 35:201
122. Pillai V, Kumar P, Hou MJ, Ayyub P, Shah DO (1995) Adv Colloid Interf Sci 55:241
123. O'Sullivan EC, Patel RC, Ward AJI (1991) J Colloid Interf Sci 146:58
124. Friberg SE, Yang CC, Sjoblom J (1992) Langmuir 8:372
125. Friberg SE, Jones SM, Yang CC, Sjoblom J (1992) J Disper Sci Technol 13:65
126. Jones SM, Friberg SE (1992) J Disper Sci Technol 13:669
127. Pileni MP (1993) J Phys Chem 97:6961
128. O'Sullivan EC, Ward AJI, Budd T (1994) Langmuir 10:2985
129. Gan LM, Zhang K, Chew CH (1996) Colloid Surface A 110:199
130. Chabra V, Ayyub P, Chattopadhyay S, Maitra AN (1996) Mater Lett 26:21
131. Fang JY, Wang J, Ng SC, Chew CH, Gan LM (1997) Nanostruct Mater 8:499
132. Liu XY, Wang J, Gan LM, Ng SC, Ding J (1998) J Magn Magn Mater 184:344
133. Adair JH, Li T, Kido T, Havey K, Moon J, Mecholsky J, Morrone A, Talham DR, Ludwig MN, Wang L (1998) Mater Sci Eng R23:139
134. Zhang K, Chew CH, Xu GQ, Wang J, LM Gan (1999) Langmuir 15:3056
135. Zhang K, Chew CH, Kawi S, Wang J, Gan LM (2000) Catal Lett 64:179
136. Liu SH, Qian XF, Yin J, Ma XD, Yuan JY, Zhu ZK (2003) J Phys Chem Solid 64:455
137. Wang DB, Yu DB, Mo MS, Liu XM, Qian YT (2003) Solid State Commun 125:475
138. Tata M, Banerjee S, John VT, Waguespack Y, McPhersond GL (1997) Colloid Surface A 127:39
139. Li HP, Liu B, Kam CH, Lam YL, Que WX, Gan LM, Chew CH, Xu GQ (2000) Opt Mater 14:321
140. Fu XA, Qutubuddin S (2001) Colloid Surface A 179:65
141. Liu B, Xu GQ, Gan LM, Chew CH, Li WS, Shen ZX (2001) J Appl Phys 89:1059
142. Liu B, Chew CH, Gan LM, Xu GQ, Li HP, Lam YL, Kam CH, Que WX (2001) J Mater Res 16:1644
143. Gan LM, Liu B, Chew CH, Xu SJ, Chua SJ, Loy GL, Xu GQ (1997) Langmuir 13:6427
144. Yee KL (1998) Masters Thesis, National University of Singapore, Singapore
145. Liu XY, Wang J, Gan LM, Ng SC, Ding J (1998) J Magn Magn Mater 184:344
146. Frieberg SE, Jones SM, Sjoblom J (1994) J Mater Synth Proces 2:1994
147. Jones SM, Frieberg SE (1995) J Non-Cryst Solids 181:39
148. Chang CL, Fogler HS (1996) AICHE J 42:3153
149. Chang CL, Fogler HS (1997) Langmuir 13:3295
150. Arriagada FJ, Osseo-Asare K (1992) Colloid Surface 69:105
151. Arriagada FJ, Osseo-Asare K (1995) J Colloid Interf Sci 170:8
152. Gan LM, Zhang K, Chew CH (1996) Colloid Surface A 110:199
153. Zhang K, Gan LM, Chew CH, Gan LH (1997) Mater Chem Phys 47:164
154. Schlag S, Eicke H-F, Mathys D, Guggenheim R (1994) Langmuir 10:3357
155. LM Gan, Zhang LH, Chan HSO, Chew CH, Loo BH (1996) J Mater Sci 31:1071
156. Kusakabe K, Yamaki T, Maeda H, Morooka S (1993) ACS Prepr 38:352

157. Kawai T, Fujino A, Kon-no K (1996) Colloid Surface 109:245
158. Wang J, Ee LS, Ng SC, Chew CH, Gan LM (1997) Mater Lett 30:119
159. Fang J, Wang J, Ng SC, Gan LM, Chew CH (1998) Ceram Int 24:507
160. Fang J, Wang J, Ng SC, Gan LM, Quek CH, Chew CH (1998) Mater Lett 36:179
161. Ee LS, Wang, Ng SC, Gan LM (1998) Mater Res Bull 33:1045
162. Lim GK, Wang J, Ng SC, Chew CH, Gan LM (1997) Biomaterials 18:1433
163. Lim GK, Wang J, Ng SC, Gan LM (1999) Langmuir 15:7472
164. Liu ZL, Lee JY, Han M, Chen WX, Gan LM (2002) J Mater Chem 12:2453
165. Gan LM, Zhang LH, Chan HSO, Chew CH (1995) Mater Chem Phys 40:94

Received: September 2003